JOURNAL OF NEUROPHYSIOLOGY
Vol. 68, No. 5, November 1992. *Printed in U.S.A.*

Experimental Tests of a Superposition Hypothesis to Explain the Relationship Between the Vestibuloocular Reflex and Smooth Pursuit During Horizontal Combined Eye-Head Tracking in Humans

WILLIAM P. HUEBNER, R. JOHN LEIGH, SCOTT H. SEIDMAN, CECIL W. THOMAS, CARL BILLIAN, ALFRED O. DISCENNA, AND LOUIS F. DELL'OSSO
Departments of Biomedical Engineering, Neurology, Neuroscience, and Otolaryngology, Case Western Reserve University, University Hospitals, and Department of Veterans Affairs Medical Center, Cleveland, Ohio 44106

SUMMARY AND CONCLUSIONS

1. We used a modeling approach to test the hypothesis that, in humans, the smooth pursuit (SP) system provides the primary signal for canceling the vestibuloocular reflex (VOR) during combined eye-head tracking (CEHT) of a target moving smoothly in the horizontal plane. Separate models for SP and the VOR were developed. The optimal values of parameters of the two models were calculated using measured responses of four subjects to trials of SP and the visually enhanced VOR. After optimal parameter values were specified, each model generated waveforms that accurately reflected the subjects' responses to SP and vestibular stimuli. The models were then combined into a CEHT model wherein the final eye movement command signal was generated as the linear summation of the signals from the SP and VOR pathways.

2. The SP-VOR superposition hypothesis was tested using two types of CEHT stimuli, both of which involved passive rotation of subjects in a vestibular chair. The first stimulus consisted of a "chair brake" or sudden stop of the subject's head during CEHT; the visual target continued to move. The second stimulus consisted of a sudden change from the visually enhanced VOR to CEHT ("delayed target onset" paradigm); as the vestibular chair rotated past the angular position of the stationary visual stimulus, the latter started to move in synchrony with the chair. Data collected during experiments that employed these stimuli were compared quantitatively with predictions made by the CEHT model.

3. During CEHT, when the chair was suddenly and unexpectedly stopped, the eye promptly began to move in the orbit to track the moving target. Initially, gaze velocity did not completely match target velocity, however; this finally occurred ~100 ms after the brake onset. The model did predict the prompt onset of eye-in-orbit motion after the brake, but it did not predict that gaze velocity would initially be only ~70% of target velocity. One possible explanation for this discrepancy is that VOR gain can be dynamically modulated and, during sustained CEHT, it may assume a lower value. Consequently, during CEHT, a smaller-amplitude SP signal would be needed to cancel the lower-gain VOR. This reduction of the SP signal could account for the attenuated tracking response observed immediately after the brake. We found evidence for the dynamic modulation of VOR gain by noting differences in responses to the onset and offset of head rotation in trials of the visually enhanced VOR.

4. If, during the visually enhanced VOR, the visual target suddenly began to move in synchrony with the head ("delayed target onset" paradigm), eye velocity in the head was sustained for ~130 ms (compensatory for the head motion and in the opposite direction of target motion) and then declined to zero, after which gaze velocity matched target velocity. The model accurately predicted the transition from the visually enhanced VOR to CEHT, with the dynamics of CEHT onset being similar to SP onset; however, the latency of onset of CEHT was somewhat shorter than that predicted by the model. Sections of eye velocity waveforms after, but not before, the onset of target motion exhibited "ringing" similar to that observed with SP onset. These results suggest that SP is activated only while tracking a moving target and that when subjects view a stationary target the VOR is supplemented by other visual mechanisms with simpler dynamics.

5. We conclude that a linear superposition of SP and VOR signals accounts for most, but not all, aspects of CEHT during passive rotation of subjects in a vestibular chair. We postulate that a parametric adjustment of the VOR, consisting of a reduction of gain, contributes to CEHT behavior.

INTRODUCTION

During visual fixation of an object of interest, the vestibuloocular reflex (VOR) helps to stabilize the angle of gaze and so maintains clear vision despite head perturbations that occur during natural activities (Grossman et al. 1988, 1989). If the object begins to move, however, and the subject tracks it with combined movements of eyes and head (combined eye-head tracking, or CEHT), the VOR must be overridden so that gaze can change to allow tracking of the moving target; how is this achieved? Because vestibular signals are still present on the vestibular nerve (Büttner and Waespe 1981) and on neurons in the vestibular nucleus that project to ocular motor neurons during CEHT (Chubb et al. 1984; Keller and Daniels 1975; Tomlinson and Robinson 1984), the VOR cannot be completely suppressed or disconnected. Rather, the VOR must be, at least in part, canceled by another neural signal. Possible candidates for this "cancellation signal" include: *1*) an internal smooth pursuit (SP) command (Barnes et al. 1978; Barnes and Lawson 1989; Lanman et al. 1978; Lau et al. 1978); *2*) an internal head-tracking command (Robinson 1982); and *3*) the VOR signal or some copy of it with an opposite sign (Cullen et al. 1991; Tomlinson and Robinson 1981). It is also possible that more than one mechanism is responsible for nulling the VOR during CEHT (Lisberger 1990). Thus some form of cancellation mechanism might be combined with a change in the gain of the VOR. For example, if a

subject imagines an earth-fixed target during sinusoidal rotation in darkness at 0.3 Hz, VOR gain is close to 1.0, but if the subject imagines the target rotating with him or her, the VOR gain declines to <0.4 (Barr et al. 1976). Such a "parametric modulation" might operate during CEHT (Koenig et al. 1986; McKinley and Peterson 1985); it is achieved rapidly and is different from the long-term adaptive changes brought about, for example, by wearing magnifying spectacles (Wilson and Melvill Jones 1979). Hence, several mechanisms may act to null the VOR during CEHT. Although the relative importance of these mechanisms has been investigated in monkey (Cullen et al. 1991; Lisberger 1990), the situation remains unsettled in humans. For example, some studies suggest that VOR cancellation by a SP signal is the only mechanism (e.g., Barnes and Lawson 1989), whereas others suggest that modulation of VOR gain occurs (e.g., McKinley and Peterson 1985).

One possible approach to identify the mechanism that regulates the VOR during CEHT is to apply stimuli that capitalize on the different inherent latencies of onset of SP eye movements and of the VOR. The shortest latency of a human visual-following response is ~75 ms (Gellman et al. 1990) and the latency of the SP system is typically >100 ms (Carl and Gellman 1987). On the other hand, VOR latency is ≤16 ms (Gauthier and Vercher 1990; Maas et al. 1989). This strategy was used in the monkey by Lanman and colleagues (1978) and more recently by Lisberger (1990) and Cullen et al. (1991). Lanman and colleagues showed that, when the monkey's head was suddenly braked during CEHT, the eye started to track the target within ~15 ms. This prompt initiation of eye movements could not have occurred as a response to retinal slip information, which would have taken much longer. Thus it appeared that a SP signal was already present during CEHT, and this signal may have been used to cancel the VOR. Therefore their results suggested that addition of an internal SP command signal to the VOR signal is the primary way the VOR is canceled during CEHT ("superposition hypothesis").

The goal of the present study was to quantitatively test this superposition hypothesis in human subjects. Our research strategy is summarized in Fig. 1. First, we measured the SP and vestibular responses of our subjects. Second, we developed two component models that accurately described the SP and vestibular responses. Third, we quantified the models for SP and VOR by either assigning accepted values or estimating optimal values of their parameters; in this way, the component models satisfactorily accounted for each subject's measured responses. Fourth, we fitted the models for SP and VOR together to create a model for CEHT in a way that proposes a generated eye movement results from a linear superposition of the signals from the two component systems. Finally, we compared the predictions of this model for combined eye-head tracking with our subjects' responses to CEHT stimuli that took advantage of the different response latencies of SP and the VOR. (Note that CEHT responses were used to test, but not to determine, the characteristics of the model for combined, eye-head tracking.) Through our analysis, we sought evidence to refute the superposition hypothesis. A preliminary report of these findings will be published (Leigh and Huebner 1993).

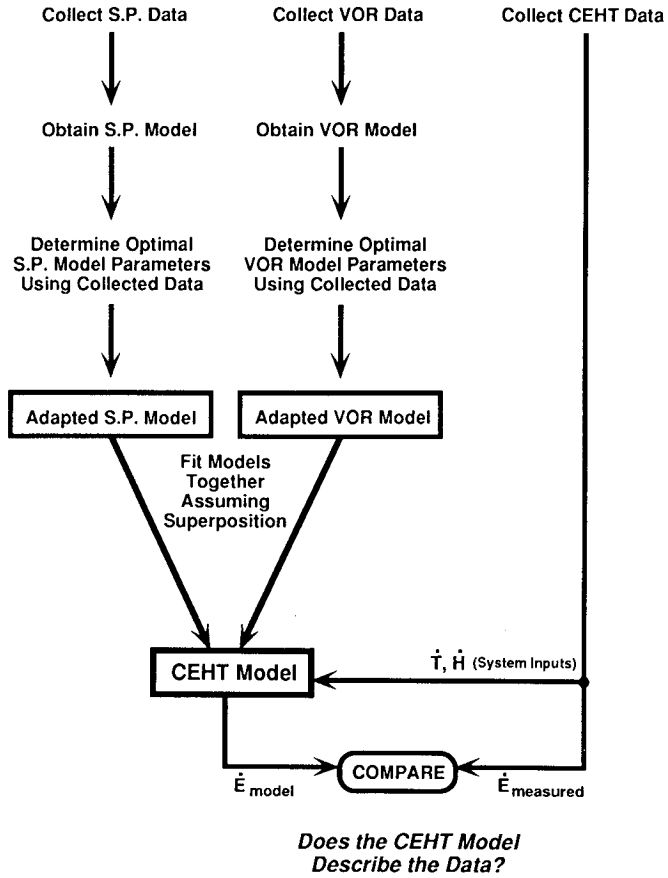

FIG. 1. Summary of overall research strategy. Smooth pursuit (SP) and vestibular responses were used to develop component models. [Combined eye-head tracking (CEHT) data were collected at the same time but were not used to develop the component models.] Next, SP and VOR models were made quantitative by either assigning accepted values or estimating optimal values of their parameters; in this way, "adapted" models satisfactorily accounted for each subject's measured SP and vestibuloocular reflex (VOR) responses. Models for SP and VOR were then combined to create a model for CEHT that proposes a generated eye movement results from a superposition of the signals from the 2 component systems. Finally, predictions of this model for CEHT were compared with subjects' responses using CEHT stimuli that took advantage of different response latencies of SP and VOR. Note that actual, recorded stimuli were used as inputs to the CEHT model, each model prediction being compared with the subject's response. Overall goal of the analysis was seek evidence to refute the superposition hypothesis for CEHT.

METHODS

Subjects and experimental equipment

We studied four normal male subjects (age range 24–42 yr); all gave informed consent. Two subjects were emmetropes, one subject was a myope who habitually wore a contact lens correction (OD −4.50, OS −5.00), and the other was a myope who habitually wore a spectacle lens correction (OD −2.00, OS −1.25 −0.50 × 006); none wore any correction during these experiments. No subject took any medication. Horizontal head (H) and gaze (G) rotations were measured using the magnetic search coil technique, with 6-ft field coils (CNC Engineering, Seattle, WA) that used a rotating magnetic vector (Collewijn 1977). Each subject wore a scleral search coil (Skalar, Delft, Netherlands) on his dominant eye; the other eye was patched. Each also wore a search coil firmly attached to his forehead to measure angular head position. Subjects sat in a 30-ft-lb vestibular chair (Templin Engineering, Laytonville, CA), with their heads firmly but comfortably

clamped to the chair's head rest, during all test paradigms. Subjects' heads were carefully positioned so that they were centered at the axis of rotation of the chair. The search coils were calibrated before each experimental session using a special protractor device.

Experimental stimuli

The visual stimulus ("target") consisted of a spot of white light projected onto a semitranslucent display screen ("tangent screen") in a darkened room. The screen was located 1.3 m in front of the subject; at this distance, it subtended approximately ±40° with respect to the subject. A slide projector was used as the light source, and its beam was passed through a small pin hole in the center of an opaque plastic slide. The resulting target subtended 0.3° and had a luminance of 0.77 ft-lamberts. The position of the visual target during a trial was programmed using a mirror galvanometer (model CCX-660, General Scanning, Watertown, MA) that was under computer control. A correction was made, in display software, so that motion of the visual stimulus across the flat screen appeared at a uniform angular velocity about the subject.

Motion of the visual stimulus consisted of 15 or 30°/s velocity steps (position ramps) applied while the subject sat facing the display screen. Each stimulus started with the visual target positioned either at zero, right 30°, or left 30°. At an unpredictable time, the stimulus would suddenly start to move and continue for a variable period ≥2 s. Data (G and target position, T) were collected from 150 ms before the onset of stimulus motion until 1 s after the target stopped.

Vestibular stimuli were also computer controlled, and chair position was monitored using an optical encoder mounted within the chair (BEI Motion Systems, Cincinnati, OH). The stimuli were programmed to be 15 or 30°/s velocity steps; the actual peak changes of velocity and peak accelerations varied between subjects and are summarized in Table 1. Onset of rotation occurred either as subjects sat directly facing the tangent screen (i.e., H was zero), or with the chair turned 30° to the right or left (H equal to ±30°). In all cases, the subject viewed the visual target whose movements are described above. During the trials in which the target remained stationary on the display screen during chair rotation, we measured the onset and offset characteristics of the visually enhanced VOR. Data (G and H) were measured from 150 ms before the rotation until 1 s after the rotation stopped. Adequate time was allowed between rotational stimuli for vestibular aftereffects to subside.

TABLE 1. *Vestibular stimuli and corresponding gaze perturbations*

Subject	$\dot{H}_p$*	$\dot{G}_p$†	$\dot{G}_p/\dot{H}_p$	$\ddot{H}_p$*	$\dot{E}_p$‡
1					
Onset	18.3 ± 0.7	4.5 ± 1.3	0.25	398 ± 66	16.6 ± 1.6
Offset	18.3 ± 0.7	1.8 ± 0.6	0.10	427 ± 110	18.5 ± 1.0
2					
Onset	19.7 ± 1.1	5.9 ± 1.3	0.30	395 ± 45	16.0 ± 2.0
Offset	19.7 ± 1.5	3.4 ± 0.8	0.17	429 ± 43	18.3 ± 1.7
3					
Onset	19.2 ± 0.8	7.0 ± 2.0	0.36	516 ± 54	15.3 ± 2.4
Offset	19.1 ± 0.5	3.8 ± 0.4	0.20	483 ± 42	18.6 ± 1.4
4					
Onset	17.4 ± 0.6	5.6 ± 1.1	0.32	391 ± 46	13.9 ± 1.9
Offset	17.6 ± 0.6	3.1 ± 0.8	0.18	396 ± 41	16.7 ± 1.8

All data were collected with head position close to zero. $\dot{H}_p$, peak head velocity (deg/s); $\dot{G}_p$, peak gaze velocity (deg/s); $\ddot{H}_p$, peak head acceleration (deg/s^2); $\dot{E}_p$, peak eye-in-orbit velocity (deg/s). * No significant difference between onset and offset values for any subject. † No overlap of onset and offset values from *subjects 1* and *3*; differences between onset and offset values for *subjects 2* and *4* were statistically significant ($P < 0.012$). ‡ Differences between onset and offset values were statistically significant for all subjects ($P < 0.05$).

Experimental paradigms

This study focused on trials in which either the target, the chair, or both rotated at 15°/s. To determine the values of parameters for the SP and VOR models, we measured responses to both the onset and the subsequent offset of the appropriate stimulus (target motion for SP and chair motion for visually enhanced VOR) while the other stimulus remained stationary. This helped ensure that each model could adequately simulate both the onset and offset activity of its associated behavior, so that any possible deviations between measured data and CEHT model predictions could not be attributed to incomplete characterization of the component models.

Two paradigms were used to test the model for CEHT; both used combined visual and (passive) vestibular stimuli. The first was the "chair brake" stimulus, which is summarized in Fig. 2*A*. Before the onset of the stimulus, head (chair) and target position were both set at either right or left 30°. After a randomized period, both chair and target began to rotate toward zero position at 15°/s. To compensate for the delay (due to inertia) before the chair began to rotate, we delayed the target onset by a corresponding period, determined empirically; thus, chair and target moved in synchrony. As the chair reached zero position, it was braked to 0°/s, but the target continued to move at the same velocity for at least 2 additional seconds.

The second stimulus, called "delayed target onset," is summarized in Fig. 2*B*. It commenced after the chair was turned right or left 30°, while the subject viewed the target light at 0°. After a variable waiting period, the chair began to turn at 15°/s toward zero. As the chair passed zero position, the target began to move in synchrony with the chair, and continued to do so for ≥2 s.

These two stimuli involving CEHT constitute the focus of this paper. In addition, some trials commenced similarly to these stimuli, but either changed direction at 0°, maintained chair motion through 0°, or did not entail target motion at all. Furthermore, by intermixing CEHT stimuli with the visual and vestibular stimuli described above, and by using trials with stimuli at 15 or 30°/s, we minimized the effects of prediction and anticipation. Subjects were encouraged to remain alert throughout the testing and were instructed to look at the visual target and follow it if it moved.

Data collection and processing

T, H, and G position signals were filtered with analog Butterworth filters (Krohn-Hite, Avon, MA), which had a bandwidth of 0–100 Hz, before digitization with 16-bit resolution at ~1,000 Hz. Responses from each subject were analyzed interactively using ASYST software (Hary et al. 1987) running on a 286 DOS-based personal computer. Data contaminated with blinks that occurred early in the record or obscured the major dynamic characteristics of the eye movement were discarded. In addition, any responses that might show any anticipatory drifts (Kowler et al. 1984) were rejected; in practice, very few responses showed what might be construed as such anticipatory eye movements.

Because we used a display screen nearer than optical infinity, a small modification to the measured data was made to adjust for the effects of the eccentric position of the eyes in the head (Huebner et al. 1992). We first measured parameters of the head geometry of each subject to quantify eye eccentricity. We then standardized the subjects' eye movement records, for each trial, to correspond to the eye rotations that would occur if the eye were instead located at the axis of rotation of the head. This modification allowed direct comparison of trials in which the head moved

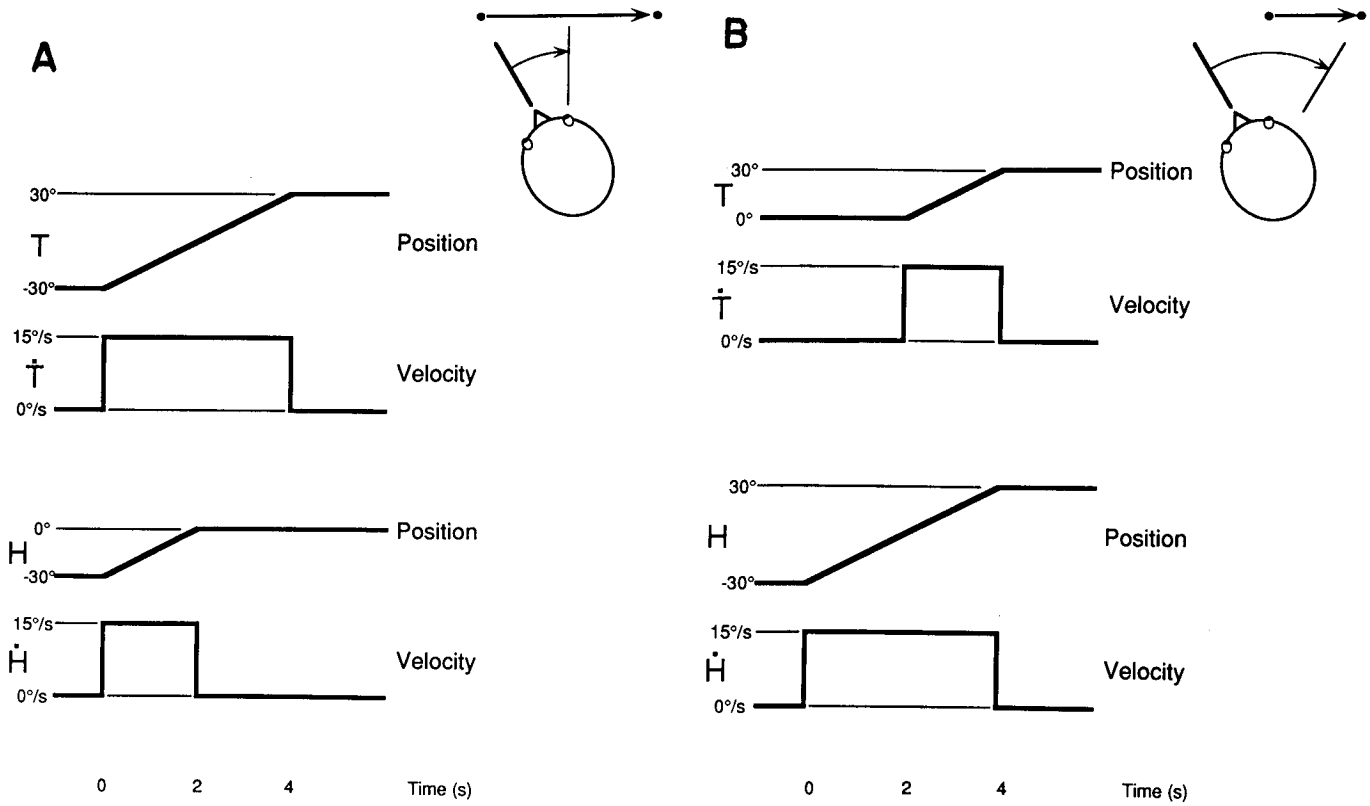

FIG. 2. Two experimental paradigms used to test the model for CEHT. *A*: chair brake. After CEHT is initiated, chair is abruptly stopped or "braked," while target continues moving. *B*: delayed target onset. After a period of visually enhanced VOR stimulation, CEHT is initiated when target motion commences. T, target position; $\dot{T}$, target velocity; H, head position; $\dot{H}$, head velocity. In this and following figures, upward/positive deflections denote rightward rotations.

with trials in which the head was stationary. Also, data collected from different subjects could then be directly compared.

Next, saccades were removed interactively from each gaze position record before filtering and differentiation; this helped minimize the "ringing" that results when high-velocity saccadic transients are processed with digital techniques. Because saccades are easier to delineate when presented in velocity data, both gaze position and the corresponding unfiltered, digitally differentiated, gaze velocity waveforms were displayed together to help the user precisely identify the limits of each saccadic fast phase. After a saccade was outlined in the velocity waveform, it was replaced with a best-fit line segment matching the data on either side of the saccade; the equation for this line was integrated to fill the corresponding gap in the gaze position waveform with a parabolic arc. Finally, the postsaccade gaze position data were offset to maintain continuity with the arc placed in the saccade gap. The unfiltered gaze velocity waveform was then discarded.

After saccade removal, the T, H, and G signals for each response were subjected to digital filtering using Chebychev Type II low-pass filters designed with nulls to occur at frequencies corresponding to coherent noise on the coil signals (Huebner et al. 1988; Thomas et al. 1988); nulls were specified at 45.85 Hz (a magnetic coil artifact), and at 60 and 120 Hz (powerline noise). This arrangement of filters attenuated most of the noise in the signals yet maintained a signal bandwidth of roughly 0–80 Hz. Data were then digitally differentiated using a two-point central-difference algorithm (Bahill and MacDonald 1983). We verified that this simple differentiation scheme provided sufficient bandwidth for our data. In this way, we obtained target velocity ($\dot{T}$), gaze velocity ($\dot{G}$), and head velocity ($\dot{H}$) and, by subtracting $\dot{H}$ from $\dot{G}$, eye-in-head velocity ($\dot{E}$).

PARAMETER ESTIMATION. After defining model structures to characterize SP and vestibular eye movement responses (described below), subject data were used to calculate optimal values of the specified model parameters using a nonlinear technique described in detail elsewhere (Huebner et al. 1990). Because the experimental stimuli, particularly the chair rotations, varied slightly from trial to trial, we used measured values of $\dot{H}$ and $\dot{T}$ as inputs to the models during the parameter estimation process. (Because of computer memory constraints, these input waveforms had an effective sample spacing of 5 ms.) Average values of parameters were calculated separately for leftward and rightward motion, for each subject; this controlled for possible directional asymmetries exhibited by the subjects.

EVALUATION OF MODEL SIMULATIONS. We tested the component SP and vestibular models, as well as the combined model for CEHT, by comparing simulations generated by the models with actual subject data. Specifically, each component model was equipped with mean parameter values for each subject, in the appropriate directions of stimuli motion. Then, for any particular SP, vestibular, chair-brake, or delayed target onset response, the appropriate model was subjected to the same combination of target and head motion waveforms (recorded during the experiment) that were applied to the subject. In this way, any idiosyncratic alterations in the stimulus waveforms were taken into account; identical stimuli were applied to the subject and the model. If constructed correctly, the component models should accurately simulate the subjects' responses. Likewise, if the component models are combined correctly and the superposition hypothesis is correct, the model for CEHT should accurately predict subjects' responses to the chair-brake and delayed target onset stimuli.

Initial comparison involved looking for certain qualitative features (e.g., presence of "ringing" in SP responses; initiation of eye movements immediately after onset of the chair brake, suggesting an active SP system). This was followed by the use of two analytic techniques: an examination of the residual arrays and a correlation analysis of critical regions of the response.

The first quantitative comparison involved calculating residual arrays, which consisted of point-by-point differences between the model's simulation and the subject's response. Averaging the residual arrays for responses in one direction of motion (leftward or rightward) for each subject (corresponding to one set of parameter values) emphasizes systematic differences between model predictions and subjects' responses, while allowing differences due to random effects to cancel each other. This method is a sensitive and detailed way to evaluate our model's predictions.

A second quantitative evaluation was made using a form of correlation analysis in which model simulations and subjects' response data values were compared directly, point by point, over a finite time interval. The degree of correlation between the two waveforms was estimated using the Pearson correlation coefficient (r). As long as analysis was restricted to the critical "transition regions" of the responses (i.e., the time intervals that focus on the specific response dynamics caused by a stimulus perturbation), the degree of correlation between a measured response and the corresponding model simulation reflected the capacity of the model to characterize the underlying process. The choice of the size of the transition region is critical: if calculations of r are performed using several data points both before the perturbation and after the model attains steady-state (relative to the number of points in the transition region), then the response data indicating poor model performance will be overwhelmed by the values at the ends of the response, and the calculated correlation values will be erroneously high. For this reason, we limited the range of the response data over which the statistics were calculated to entail only the anticipated transition region, because this is where the model is most likely to fail. To be certain that we were working with as much of the transition region as possible, we made the actual choice of the transition region size for each paradigm on the basis of observations of various measured responses. For the VOR onset, VOR offset, and chair brake paradigms, we used only the model and response data from the first 100 ms after the chair began to change velocity. Because subjects took varying amounts of time to reach peak eye velocity in response to the onset of target motion, we used from 350 to 400 ms after the target began to move, depending on the subject, for the SP onset and delayed target onset paradigms. Finally, we used the first 600 ms after the onset of target motion to evaluate the performance of the SP offset model in describing subject response data.

RESULTS

SP and vestibular testing

Here we describe the results of testing the SP and visually enhanced VOR responses, summarizing the salient features that the component SP and VOR models had to simulate before a superposition model for CEHT could be constructed.

A typical SP onset response is shown in Fig. 3. After a latency of ~130 ms, the eye starts to accelerate, but eye velocity overshoots and then oscillates about target velocity. Figure 3 also shows a typical offset of SP. Note how the response consists essentially of a simple, negative exponential decay of eye velocity, with only slight overshoot. These features, which were present in all of our subjects, are characteristic of SP responses and have been described and analyzed previously by Robinson and colleagues (1986). This response morphology suggested that separate mechanisms govern the onset and offset of smooth pursuit, and it was postulated (Luebke and Robinson 1988) that the response to cessation of target motion was performed by a separate SP offset or "visual fixation" system.

During initial analysis of our vestibular data, we observed a novel phenomenon that we needed to account for in our model of the visually enhanced VOR: the perturbation of gaze produced at the onset of head rotation was consistently greater than at the offset. Typical onset and offset responses are shown in Fig. 4. The velocity plot in Fig. 4*A* shows the complete response to a 15°/s head rotation starting at left 30° and moving to 0°, where the chair suddenly stopped; the target remained stationary at 0° throughout. Note that the gaze perturbation is greater at the onset of head rotation than at the offset. In Fig. 4*B*, the response to the onset of chair rotation, starting at 0° (*left*) is compared with the response to the offset of a different trial at 0° (*right*) that had started with the head at left 30°. The temporal profiles and magnitudes of these "on" and "off" head perturbations are shown to be very similar, and so a direct comparison of their gaze perturbations is possible.

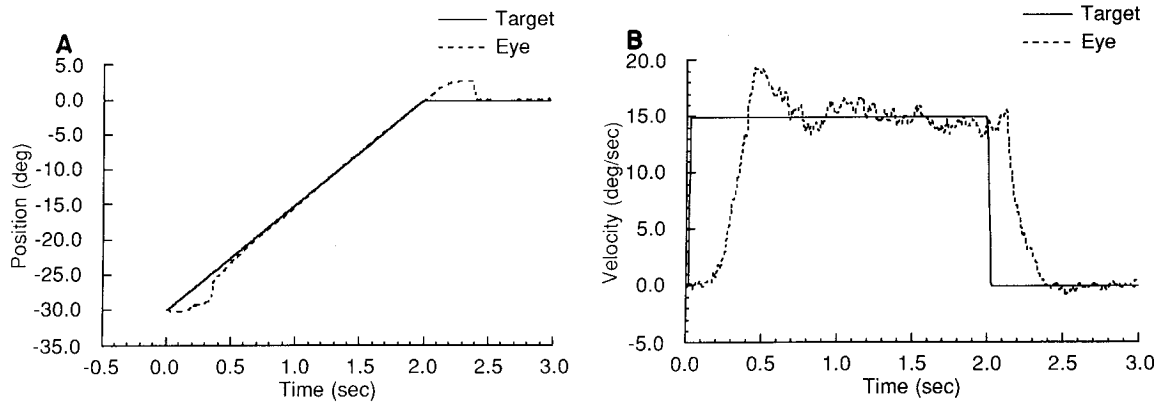

FIG. 3. Typical example of SP onset and offset, from *subject 1*. *A*: position records. *B*: velocity records, after removal of saccades (see text). Onset of SP is characterized by eye velocity overshooting target velocity and subsequently "ringing." In contrast, the offset of SP essentially consists of a simple, negative exponential decay of eye velocity, with only slight overshoot.

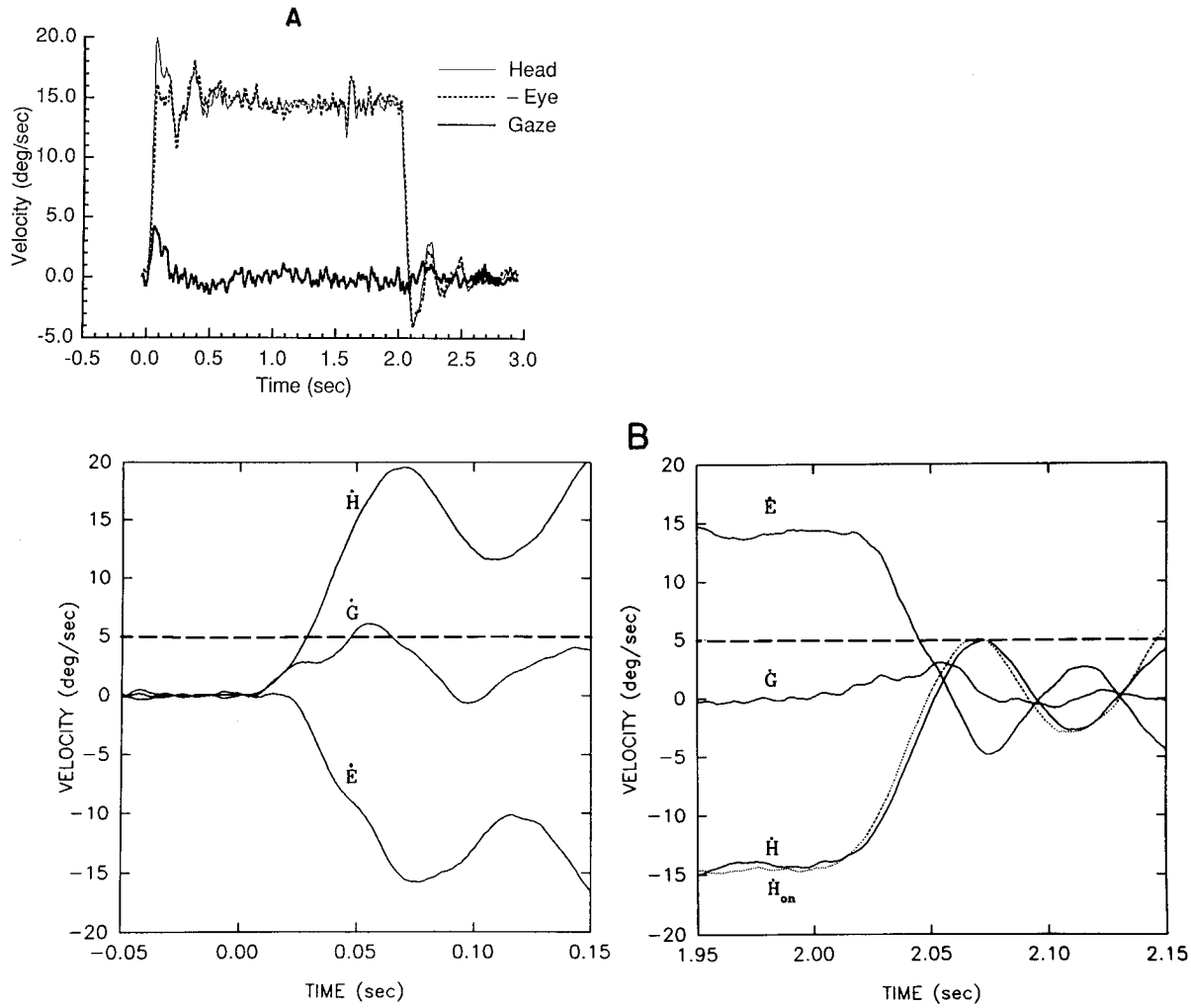

FIG. 4. Typical example of the visually enhanced VOR. *A*: complete response from *subject 1*. Note that eye velocity is inverted (−Eye) to allow direct comparison with head velocity. Gaze velocity is perturbed more at onset than at offset of head rotation. *B*: comparison of onset (*left*) and offset (*right*) of 2 separate responses from *subject 3*, both changes of head velocity occurring in the same direction. For purposes of comparison, the waveform of the onset head rotation ($\dot{H}_{on}$, shown as a · · ·) has been transposed and replotted to compare it with the offset waveform (*B, right*). Note that although changes in head velocity at onset and offset have very similar magnitude and dynamic characteristics, gaze velocity is perturbed >5°/s at onset, but not at offset. Time scales are different for *A* and *B*.

The initial perturbation of gaze after the change of head velocity is similar for both responses and reflects the overall latency to onset of the VOR. The two gaze velocity records subsequently show profiles that are similar qualitatively but different quantitatively; the gaze perturbation during onset of head rotation is greater than that during offset. This difference in the perturbation of gaze is caused by dissimilar changes in eye velocity occurring in response to the changes in head velocity. Accounting for this finding was the major challenge in our subsequent modeling of the VOR.

The dynamic characteristics of the stimuli and the peak gaze velocities ($\dot{G}_p$) produced are summarized in Table 1, for each subject. (So as not to confound these data with possible effects due to initial eye-in-orbit position, all measurements given in Table 1 were made with the chair either starting or stopping at 0°.) Although there were no significant differences between the peak head velocities (and accelerations) for motion onset and offset, gaze perturbations during head rotation onset were, on average, 53% greater than during offset. Two subjects (*1* and *3*) showed no overlap of values of $\dot{G}_p$; the gaze perturbation was always greater during the onset of head rotation. The other two subjects each showed only one data point of overlap, and the values of $\dot{G}_p$ at onset were significantly greater than at offset ($P < 0.012$) when compared using Wilcoxon's test. The peak values of $\dot{E}$ were also significantly different for onset and offset stimuli ($P < 0.05$). Because similar changes in head movement resulted in dissimilar eye movement responses, we believe that the increased gaze perturbations at rotation onset may be attributed to a lower resting VOR gain (see below).

In control experiments we determined that the onset-offset perturbation difference was still present when rotations started with the eye at a central (0°) or an eccentric position (30°) in the orbit; thus the orbital position of the eye did not affect this observed perturbation effect. Furthermore, the perturbation difference was still present when 30°/s velocity steps were applied. We also took great pains to

randomize stimuli and, for example, subjects did not know whether the chair would stop or change direction as it reached the 0° position or whether the visual stimulus would move. Hence, the effects of prediction in these responses were minimized. Attempts to demonstrate an onset-offset asymmetry by imposing a second velocity-step increase 2 s after the first or by using manual, high-acceleration chair turns were confounded by difficulties in producing pairs of stimuli (i.e., at both the onset and offset of rotation) that were as closely matched temporally (i.e., in acceleration and frequency components) as were the present stimuli. Qualitatively, similar results were produced, but direct comparison was not possible.

Three of the four subjects showed $\dot{G}_p$ perturbations ~60 ms after the onset of head rotation; the perturbations were largely over within 200 ms. Although the SP or other visual tracking systems (Gellman et al. 1990) may have contributed to this recovery, much of the decline in $\dot{G}$ was evident before such systems could act. Moreover, the smaller perturbation of gaze at the offset of rotation could not be explained by visual mechanisms because the time delay involved in visual processing would not allow for instantaneous correction of retinal errors. Thus we propose that VOR gain changes depending on the state of head motion: the gain may assume a lower level while the head is at rest and then subsequently increase after the onset of head motion.

Development of a model for CEHT

This section describes in three parts our procedure for constructing the CEHT model and testing the superposition hypothesis: *1*) synthesis of component models for the SP and visually enhanced VOR responses; *2*) determination of optimal values of parameters of these two component models; *3*) combining of the models for SP and VOR to create a model for CEHT in a way that proposes a generated eye movement results from a superposition of the signals from the two component systems.

SYNTHESIS OF MODELS FOR SP AND VOR. The model we used to describe both the onset and offset of SP is an extension of the one proposed for human subjects by Robinson and colleagues (1986), shown in Fig. 5. Although other valid models of SP exist and may have been used (e.g., Krauzlis and Lisberger 1989), the model of Robinson et al. proved to satisfactorily describe our human data and was well suited for use in the subsequent parameter estimation process. Using techniques described elsewhere (Huebner et al. 1990), we used measured data to determine optimal values for six parameters of the SP onset model: the loop gain, A; the time constant of the central processing lag element, T_c; the piecewise-linear breakpoint in the acceleration-saturation element, $\dot{e}_0$; the plasticity parameter governing overall response gain, P_1; the central delay element, τ_1; and the internal feedback delay, τ_3. Optimizing these six parameters yielded model simulations morphologically similar to the underlying response data. Following the work of Goldstein (1987), if we can assume that the inherent neural integration of the ocular motor command signal is performed with dynamics that can be described using a "pulse-slide-step" integrator model, and if we assume that the ocular motor plant can be characterized with a two viscoelastic element model, then the overall integrator-plant dynamics can be reduced to simple integration. However, because our models maintain the eye movement signals in terms of velocity, this integration is removed from the models and is left as an assumed operation (see Robinson et al. 1986). Thus, by making these assumptions about the neural integrator and

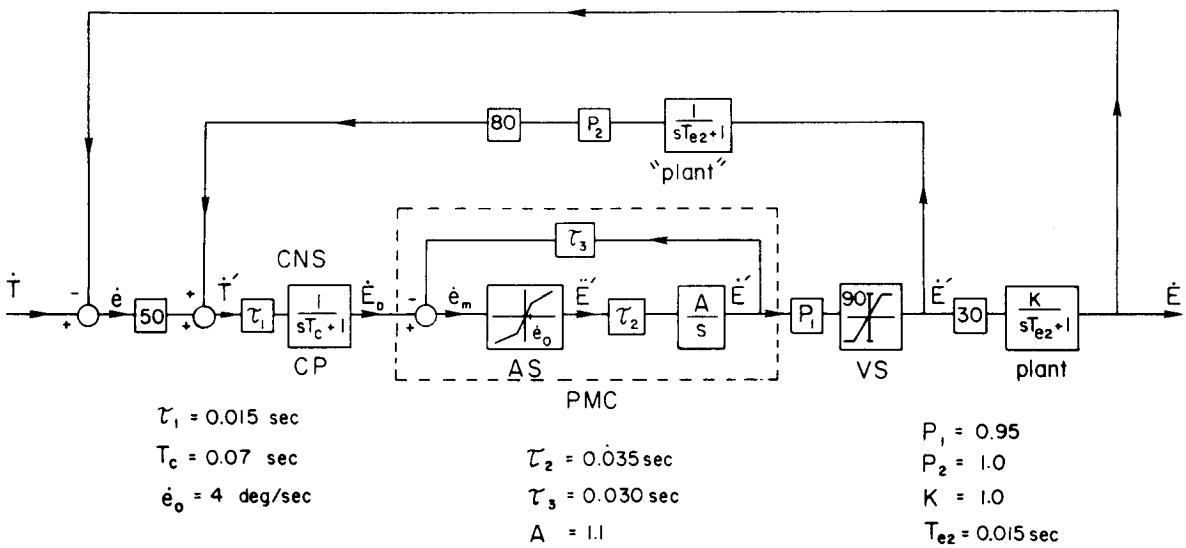

FIG. 5. A model for SP onset, proposed by Robinson et al. (1986), and parameter values used. CP, central processing felt to reflect activity of the CNS; PMC, premotor circuitry; AS, acceleration saturation; VS, velocity saturation; $\dot{T}$, target velocity (input); $\dot{E}$, eye velocity (output); $\dot{e}$, retinal error velocity; $\dot{T}'$, centrally reconstructed copy of target velocity; $\dot{E}_D$, desired eye velocity; $\dot{e}_m$, motor error; $\ddot{E}'$, desired eye acceleration; $\dot{E}'$, eye velocity command signal; numbers in boxes refer to the number of ms of pure delay; τ_1, τ_2, and τ_3, internal delays; T_c, time constant of CP; $\dot{e}_o$, break in nonlinearity AS; A, PMC loop gain; K, gain of the ocular motor plant; T_{e2}, time constant of ocular motor plant; P_1 and P_2, plasticity gain parameters. Input-output relation of AS is $\ddot{E}' = 40 + 5\dot{e}_m$, $|\dot{e}_m| > \dot{e}_o$; $\ddot{E}' = (5 + 40/\dot{e}_o)\dot{e}_m$, $|\dot{e}_m| < \dot{e}_o$. Reproduced with permission.

the plant, we have effectively eliminated the need to add special dynamics to describe the plant (Goldstein 1983). Therefore, although elements labeled "Plant" are shown in our models, they are included only for completeness and do not contribute to the overall model dynamics. Also, any delay in the plant could be distributed to, or recombined from, other system delay elements, as necessary.

Because some of our experimental trials involved stopping the motion of the visual target, we augmented the SP model in a way that describes SP offset as well as onset (Fig. 6). Robinson et al. (1986) noted that separate mechanisms govern the onset and offset of SP, and whereas SP onset often exhibits overshoot and ringing of the velocity waveform, SP offset usually declines monotonically toward zero with a time course that could be described by an exponential with a single time constant. Our SP offset data were consistent with this observation. Thus we added to the SP model a separate pathway that was comprised of a time-delay element in series with a single-pole phase-lag element to describe SP offset. To use this model, we needed to estimate values for the time constant of the lag, T_f, and of the delay element, τ_f. The output of the overall SP model was then derived from either the onset or the offset pathway, depending on the brain's internal representation of target velocity: if the target were moving, the brain would use the onset pathway; if target fell below some threshold value (here set to 5°/s), the brain would use the signal from the offset pathway. Although this value is somewhat higher than the threshold of SP onset reported by Luebke and Robinson (1988) and may seem arbitrary, it encompasses the range of slip of images across the retina that may occur during natural head motion when the subject fixates upon a stationary target (Grossman et al. 1989; Steinman and Collewijn

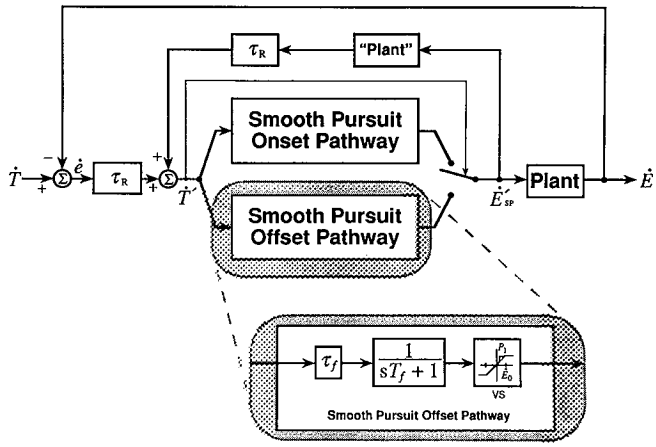

FIG. 6. Complete model for SP combining pathways for both onset and offset of pursuit. SP onset pathway is derived primarily from the model of Robinson et al. (1986) in Fig. 5, whereas the model pathway for the offset of SP consists of a lag element, with a time constant T_f, in series with a delay, τ_f; s is the Laplace complex frequency operator. A velocity saturation element, VS, was included to make the offset pathway comparable with the model for SP onset; however, this element did not influence our subjects' responses to 15°/s stimuli. Target velocity ($\dot{T}$) and eye-in-orbit velocity ($\dot{E}$) are compared at the retina (denoted by the leftmost summing junction) to obtain retinal error velocity ($\dot{e}$). Model responds to a representation of target velocity ($\dot{T}'$) that is recreated internally by combining retinal error velocity ($\dot{e}$) with an efference copy of eye-in-orbit velocity ($\dot{E}'_{SP}$). The latter requires that properties of the ocular motor plant ("Plant") and visual delays (τ_R) be taken into account (see Robinson et al. 1986 for a detailed discussion of this). If the value of $\dot{T}'$ falls below 5°/s, the brain stops monitoring the signal from the pursuit onset and begins to derive the command signal from the pursuit offset pathway (indicated by arrow to switch, at *right*).

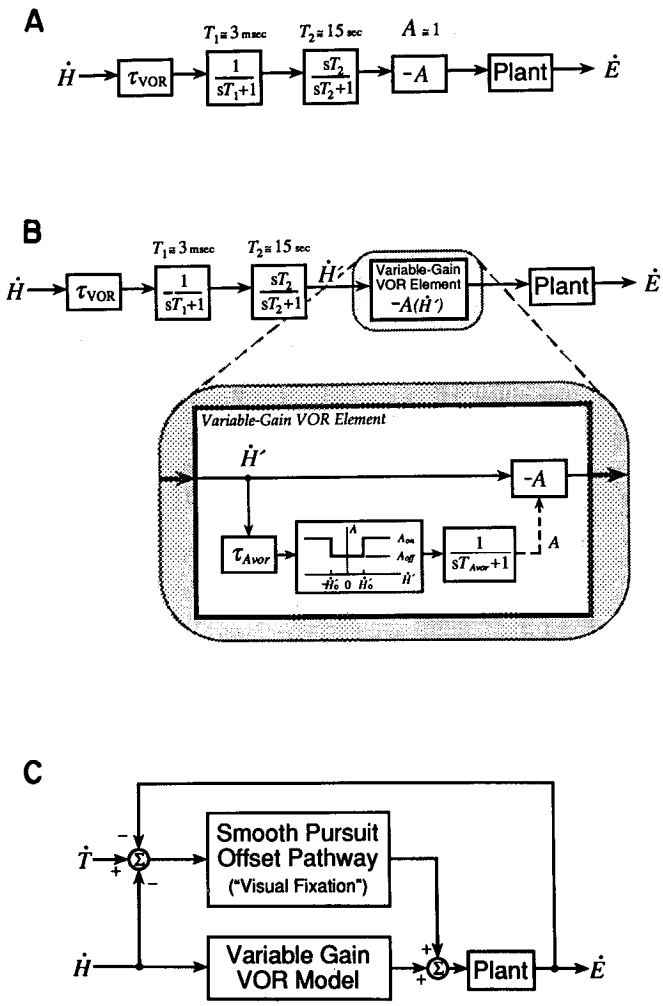

FIG. 7. VOR models. *A*: "elementary" model consisting of lag and lead elements, governed by the parameters T_1 and T_2, that represent known dynamics of the semicircular canals. "Short" time constant of the VOR, T_1, is due to hydrodynamic properties of the endolymph, and was set to 3 ms. "Long" time constant, T_2, was determined experimentally for each subject from the time course of decay of postrotational nystagmus in darkness. A delay element, τ_{vor}, helped account for the latency of the VOR. A gain element −A determined the magnitude of eye rotations that occur in the direction opposite to head rotations. $\dot{E}$, eye-in-orbit velocity; $\dot{H}$, head velocity. *B*: model of the VOR with a variable gain that is adjusted according to the magnitude of an internal head velocity signal, $\dot{H}'$. If the magnitude of the internal head velocity signal was less than some threshold value, $\dot{H}'_o$ (which we arbitrarily set to 5°/s), then the VOR gain was set to the "resting" value A_{off}. On the other hand, if the magnitude of the internal head velocity signal rose to greater than $\dot{H}'_o$, then VOR gain increased to the "active" value of A_{on}. A delay element τ_{Avor} allowed time for the brain to make decisions about which level to set the VOR gain; a lag element, governed by the time constant T_{Avor}, made the change of VOR gain gradual. *C*: scheme for modeling the visually enhanced VOR. To account for the visual contributions to eye movements during the visually enhanced VOR, we supplemented the variable-gain VOR model in *B* with the portion of the SP model responsible for maintaining fixation on a stationary target (the SP offset pathway, shown in Fig. 6). Although not explicitly shown, this scheme incorporated a feedback loop conveying an efference copy of eye-in-orbit velocity as part of the SP offset pathway, similar to that shown in Fig. 6.

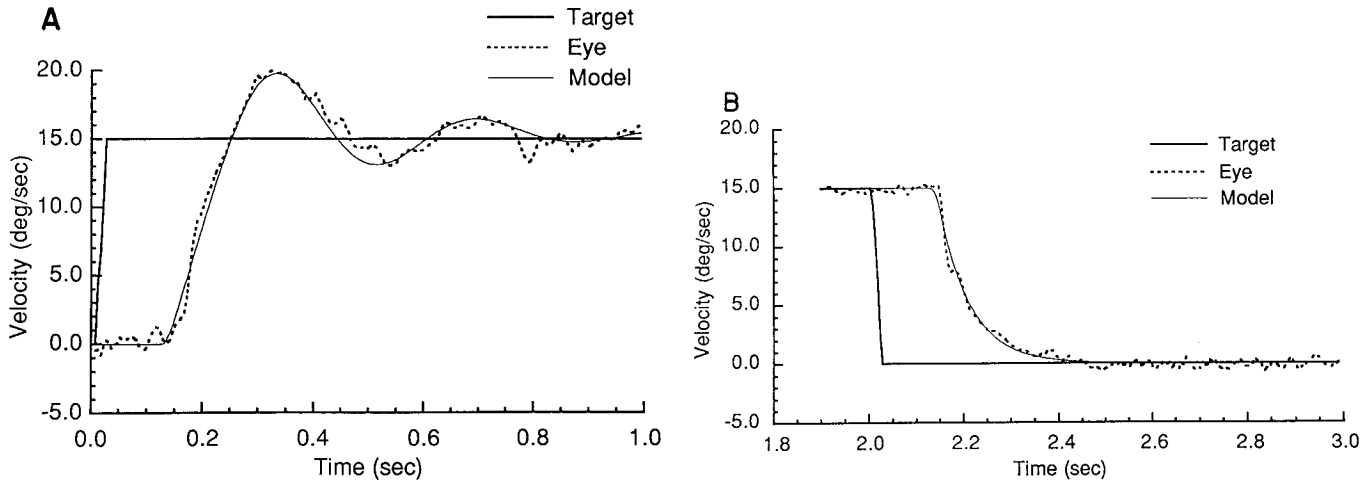

FIG. 8. *A*: comparison of a typical SP onset response from *subject 1* and the corresponding simulation of the response by the SP onset model, using optimal parameter values. *B*: comparison of a typical SP offset response from *subject 1* and the corresponding simulation of the response by the SP offset model, using optimal parameter values.

1980). Although the brain may not process SP signals in quite this manner, the scheme did satisfactorily describe our SP onset and offset data.

To simulate the perturbations of gaze that occur in response to the onset and offset of 15°/s steps of head velocity while the subject fixates a stationary target, we started by constructing a simple model of the VOR, based on currently accepted schemes (Robinson 1981; Wilson and Melvill Jones 1979) (Fig. 7*A*). It consisted of lag and lead elements, governed by the parameters T_1 and T_2, that represent known dynamics of the semicircular canals. The lag element limits the bandwidth of these VOR transducers; the value of its time constant, T_1, is ~3 ms (Wilson and Melvill Jones 1979). The "long" time constant of the canals, T_2, which is attributed to the elastic properties of the cupula, has been estimated indirectly to be ~5 s (Cohen et al. 1981). On the other hand, the predominant time constant of the entire VOR (estimated, for example, from the

TABLE 2. *Mean optimal values of parameters of smooth pursuit onset and offset*

	A	T_c	$\dot{e}_0$	P_1	τ_3	τ_1	τ_f	T_f
Subject 1								
Rightward	1.219	0.043	9.664	1.004	0.047	0.036	0.055	0.081
$n_1 = 8, n_2 = 8$	(0.126)	(0.041)	(3.837)	(0.020)	(0.007)	(0.028)	(0.015)	(0.018)
Leftward	1.201	0.109	7.873	0.933	0.051	0.030	0.060	0.050
$n_1 = 5, n_2 = 8$	(0.162)	(0.024)	(2.547)	(0.023)	(0.008)	(0.021)	(0.012)	(0.022)
Lumped	1.212	0.069	8.975	0.976	0.049	0.034	0.058	0.065
$n_1 = 13, n_2 = 16$	(0.141)	(0.048)	(3.509)	(0.040)	(0.008)	(0.026)	(0.014)	(0.025)
Subject 2								
Rightward	1.136	0.031	14.225	1.014	0.052	0.049	0.083	0.088
$n_1 = 5, n_2 = 9$	(0.202)	(0.022)	(5.069)	(0.017)	(0.021)	(0.015)	(0.018)	(0.018)
Leftward	0.995	0.025	12.257	1.003	0.062	0.051	0.061	0.067
$n_1 = 6, n_2 = 9$	(0.223)	(0.018)	(3.816)	(0.028)	(0.013)	(0.023)	(0.011)	(0.015)
Lumped	1.059	0.028	13.151	1.008	0.057	0.051	0.072	0.078
$n_1 = 11, n_2 = 18$	(0.225)	(0.020)	(4.537)	(0.024)	(0.018)	(0.019)	(0.018)	(0.020)
Subject 3								
Rightward	1.006	0.082	11.565	0.980	0.064	0.019	0.048	0.104
$n_1 = 4, n_2 = 7$	(0.175)	(0.045)	(2.919)	(0.027)	(0.012)	(0.019)	(0.012)	(0.015)
Leftward	0.923	0.038	7.337	1.004	0.041	0.044	0.042	0.062
$n_1 = 6, n_2 = 6$	(0.131)	(0.037)	(5.106)	(0.031)	(0.020)	(0.028)	(0.012)	(0.012)
Lumped	0.956	0.055	9.028	0.995	0.050	0.034	0.045	0.085
$n_1 = 10, n_2 = 13$	(0.155)	(0.045)	(4.831)	(0.032)	(0.021)	(0.028)	(0.012)	(0.025)
Subject 4								
Rightward	0.912	0.001	17.058	1.068	0.096	0.073	0.064	0.058
$n_1 = 7, n_2 = 5$	(0.097)	(0.000)	(3.212)	(0.048)	(0.019)	(0.019)	(0.017)	(0.014)
Leftward	0.876	0.007	9.710	0.980	0.072	0.065	0.059	0.089
$n_1 = 5, n_2 = 4$	(0.167)	(0.007)	(7.722)	(0.019)	(0.018)	(0.023)	(0.009)	(0.010)
Lumped	0.896	0.004	13.792	1.029	0.085	0.069	0.062	0.071
$n_1 = 12, n_2 = 9$	(0.134)	(0.005)	(6.750)	(0.058)	(0.022)	(0.021)	(0.015)	(0.020)

Standard deviations listed in parentheses; time constants and delays are given in seconds. n_1, number of cases used for SP onset parameters A-τ_1; n_2, number of cases used for SP offset parameters τ_f and T_f. A, loop gain, T_c, time constant of central processing lag element; $\dot{e}_0$, piecewise-linear breakpoint in acceleration-saturation element; P_1, plasticity parameter governing overall response gain; τ_3, internal feedback delay; τ_1, central delay element; τ_f, offset delay element; T_f, time constant of offset lag (see text for details).

TABLE 3. *Mean optimal values of parameters of variable-gain VOR model*

	n	A_{off}	A_{on}	T_{Avor}	τ_{Avor}
Subject 1					
Rightward	12	0.814	0.985	0.277	0.082
		(0.064)	(0.024)	(0.420)	(0.065)
Leftward	10	0.769	0.960	0.232	0.068
		(0.128)	(0.024)	(0.303)	(0.071)
Lumped	22	0.793	0.973	0.256	0.076
		(0.101)	(0.027)	(0.372)	(0.068)
Subject 2					
Rightward	7	0.779	0.960	0.468	0.072
		(0.031)	(0.035)	(0.235)	(0.040)
Leftward	11	0.685	0.914	0.081	0.094
		(0.098)	(0.026)	(0.112)	(0.036)
Lumped	18	0.721	0.932	0.231	0.086
		(0.092)	(0.038)	(0.254)	(0.039)
Subject 3					
Rightward	12	0.771	0.990	0.358	0.079
		(0.057)	(0.019)	(0.217)	(0.070)
Leftward	5	0.863	0.977	0.175	0.033
		(0.069)	(0.022)	(0.166)	(0.034)
Lumped	17	0.798	0.986	0.304	0.066
		(0.074)	(0.021)	(0.220)	(0.065)
Subject 4					
Rightward	8	0.754	0.916	0.283	0.093
		(0.062)	(0.041)	(0.176)	(0.050)
Leftward	7	0.735	0.963	0.100	0.094
		(0.052)	(0.055)	(0.047)	(0.051)
Lumped	15	0.746	0.938	0.198	0.093
		(0.058)	(0.054)	(0.161)	(0.050)

Standard deviations listed in parentheses; time constant and delays are given in seconds. A_{off}, "resting" value of VOR gain; A_{on}, "active" value of VOR gain; T_{Avor}, lag element governing VOR gain change; τ_{Avor}, delay element governing VOR gain change (see text for details).

rate of decay of postrotational nystagmus in darkness) is closer to 15 s; this larger value is attributed to a phenomenon called "velocity storage" (Raphan et al. 1979). In this research, we were interested only in transient characteristics of the VOR. Because velocity storage influences the VOR only during sustained rotations, we excluded elements that explicitly describe velocity storage from our model to simplify subsequent parameter estimation. For our experiments, which concern the overall behavior of the VOR, we measured T_2 directly for each subject (by determining the decline of slow-phase velocity of nystagmus induced by a 60°/s velocity-step rotation in darkness); we let this parameter represent the time constant of the VOR rather than the cupula. Thus T_1 was assigned a constant value of 3 ms, whereas T_2 was measured directly for each subject and held constant during the subsequent parameter estimation procedure. A delay element, τ_{VOR}, was included in this model to account for the latency of the VOR. Finally, a gain element, $-A$, determined the magnitude of the eye rotations that occur in the direction opposite to head rotations.

Preliminary simulations, even in conjunction with the model for visually mediated responses (see below), confirmed that the observed perturbations of gaze at the onset and offset of rotation could not be achieved by the model with a fixed value for VOR gain. Therefore we modified this standard model and formulated a VOR model with a variable gain element (Fig. 7*B*) that is adjusted according to the magnitude of an internal head velocity signal, $\dot{H}'$ (Huebner and Leigh 1992). If the magnitude of the internal head velocity signal was less than some threshold value, $\dot{H}'_o$ (which we arbitrarily set to 5°/s), then the VOR gain was set to the "resting" value A_{off}. With the VOR gain substantially less than 1.0, an abrupt head movement would cause a corresponding perturbation of $\dot{G}$. On the other hand, if the magnitude of the internal head velocity signal rose to $>\dot{H}'_o$, then VOR gain increased to the "active" value A_{on}. With the active VOR gain near 1.0, only a small perturbation of G would occur when the head abruptly changed speed. A delay element τ_{Avor} was added to allow time for the brain to make decisions about which level to set the VOR gain. Also, because it seemed unreasonable to expect the VOR gain to change instantaneously, we included a lag element, governed by the time constant T_{Avor}, to make the change of VOR gain more gradual. It is interesting to note that, even when initial chair position was eccentric and the subject knew which direction he would move, the initial perturbation of $\dot{G}$ at motion onset was still significantly greater than at motion offset. This suggests that for passive head rotations it was generally not possible for subjects to preinflate their VOR gain values using prediction or anticipation.

When determining the parameters of the VOR model, it was necessary to account for the overall behavior of gaze velocity during head rotations as subjects fixated on a stationary target. This required that we develop a model for the visually enhanced VOR that incorporated both visual and vestibular mechanisms. We fulfilled this by coupling the VOR model with the offset component of the SP model (Fig. 7*C*). Thus we treated our SP offset pathway as a "visual fixation" mechanism when it was used to supplement the VOR in maintaining gaze on a stationary target during head rotation. In this configuration, the input to SP offset ("visual fixation") is target velocity with respect to the subject's gaze velocity ($\dot{T} - \dot{G}$); because the target is stationary, slip of its image across the retina is caused only by gaze perturbation; i.e., apparent target velocity is $-\dot{G}$. The output of the VOR model was added to that from the model for the visual fixation, and the combined eye movement command signal was then sent to the plant. (Again, using the reasoning outlined above for the model of SP onset, the actual dynamics of the plant may be ignored.) Finally, we used our subjects' responses (such as shown in Fig. 4) in conjunction with the model for the visually enhanced VOR (Fig. 7*C*) to estimate the optimal values of five parameters of the VOR model: τ_{VOR}, A_{off}, A_{on}, τ_{Avor}, and T_{Avor}.

DETERMINATION OF OPTIMAL PARAMETER VALUES OF SP AND VOR MODELS. Figure 8 shows a SP onset response and the corresponding simulation using the SP onset model. The parameters of the model for this simulation were those determined to be optimal for this response. The optimal values of parameters for the SP onset model are summarized in Table 2. Average values for each subject are given for both leftward and rightward responses. The optimal values of parameters in Table 2 are in general agreement with those published by Robinson and colleagues (1986).

We next tested the capacity of the SP onset model to describe subject response data when the model was equipped with the average optimal parameter values for a given subject in the appropriate stimulus direction. On in-

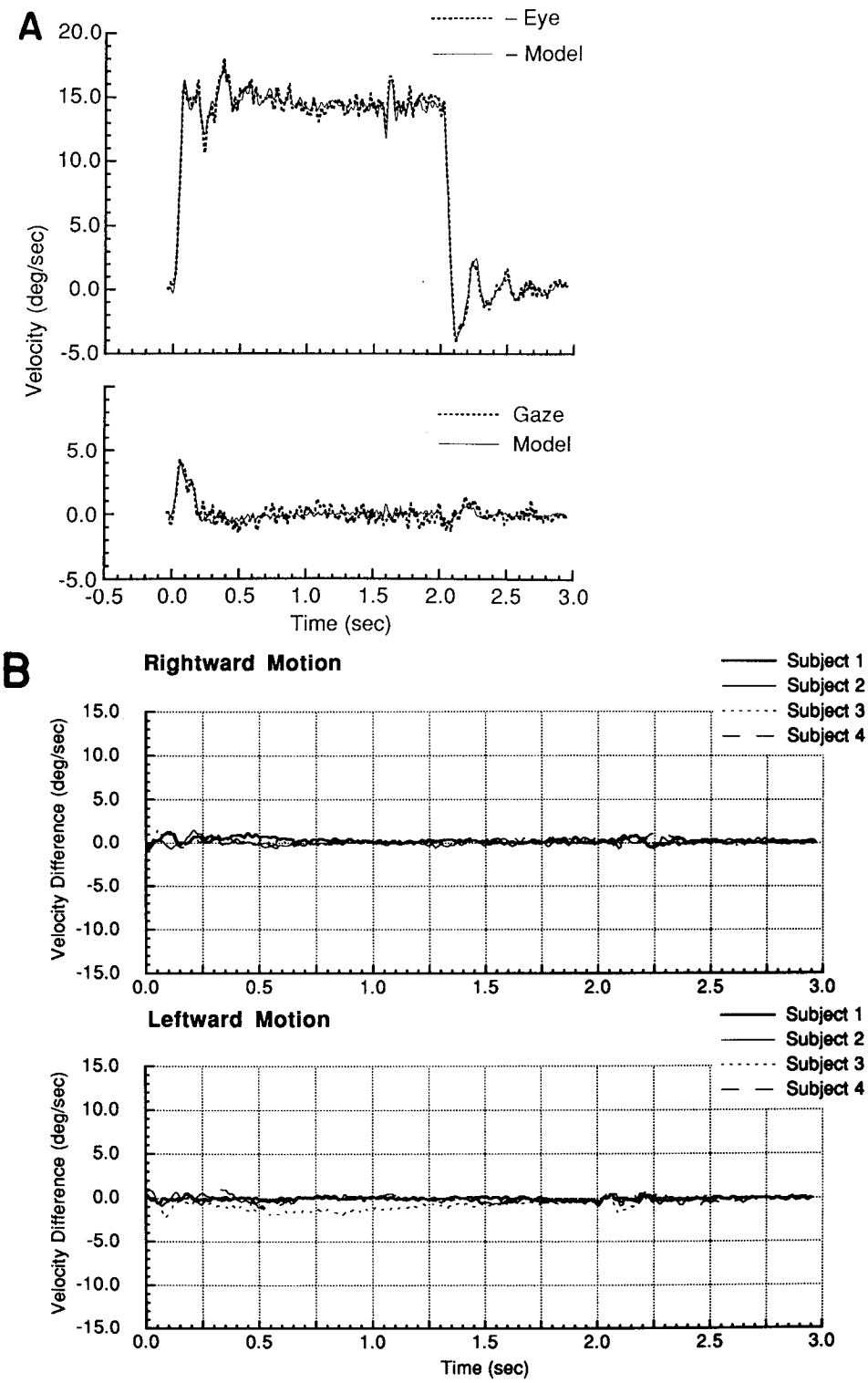

FIG. 9. *A*: comparison of a typical response of the visually enhanced VOR from *subject 1* (same response as shown in Fig. 4*A*) and the corresponding simulation of the response by the model of the visually enhanced VOR (shown in Fig. 7*C*), using optimal parameters for this subject. (Head velocity is not shown for clarity of display.) Note that eye velocity is inverted (−Eye) to allow direct comparison with the records of Fig. 4. *B*: comparison between model simulations and subjects' responses for the visually enhanced VOR made by computing average residual waveforms (see METHODS). Positive velocity values indicate that the mean subject's response exceeded the model's predictions. Deviations between model simulations and subject responses remained small at the onset and offset of head rotation. (Note that the full-scale plot range for this and subsequent residual waveform plots corresponds to the stimulus amplitude, 15°/s. This provides a consistent reference for evaluating and comparing magnitudes of observed features in residual waveforms.)

spection, the agreement between model simulations and subjects' responses was good, and the correlation coefficient was >0.98 for all subjects.

The mean values of optimal parameters for the SP offset model are also summarized in Table 2. Figure 8*B* shows a typical SP offset response along with the corresponding simulation of the SP offset, using optimal parameter values for this response. The exponential decline simulated by this simple model adequately described all of the subjects' responses. When we compared the simulations of SP offset with the measured responses from each subject, the correlation coefficient was >0.98. Thus we were able to justify incorporation of the SP model in our overall model for CEHT.

The mean values of optimal parameters for the VOR model are summarized in Table 3. First, note that the val-

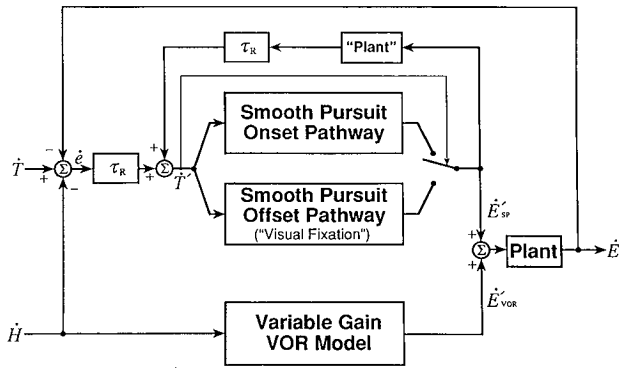

FIG. 10. A model for CEHT that assumes a superposition of vestibular and SP signals. Final eye movement command signal is simply the sum of the command signal from the variable-gain VOR model, $\dot{E}'_{VOR}$, and the command signal from the SP model, $\dot{E}'_{SP}$. Target velocity ($\dot{T}$), head velocity ($\dot{H}$), and eye-in-orbit velocity ($\dot{E}$) are compared at the retina (denoted by leftmost summing junction) to obtain retinal error velocity ($\dot{e}$). Pursuit model responds to a representation of target velocity ($\dot{T}'$) that is recreated internally by combining retinal error velocity ($\dot{e}$) with an efference copy of the SP signal ($\dot{E}'_{SP}$). The latter requires that properties of the ocular motor plant ("plant") and visual delays (τ_R) be taken into account (see Robinson et al. 1986 for a detailed discussion of this). If the value of $\dot{T}'$ falls below 5°/s, the brain stops monitoring the signal from the pursuit onset and begins to derive the command signal from the pursuit offset model (indicated by arrow to switch, at *right*).

ues of the "resting" VOR gain, A_{off}, before the onset of head rotation (group mean = 0.76) were 0.2 less than the values of the "active" gain, A_{on} (group mean = 0.96). These values range from 0.68 to 0.86 at rest and from 0.91 to 0.99 during rotation. Second, note that a reliable estimate for the pure delay element, τ_{VOR}, could not be made because of the comparably large sample spacing (5 ms) in the waveforms used for parameter estimation; the values determined were ≤1 ms, so that the dynamics of the model's simulations of VOR onset were largely determined by the "short" time constant of the semicircular canals, T_1 (3 ms), and the resting VOR gain, A_{off} (≈0.75). The overall apparent latency of the VOR was estimated interactively, as previously described (Maas et al. 1989), and mean values ranged from 7 to 11 ms. Nonetheless, the model's simulations of VOR onset sufficed for the purposes of testing the superposition model (see below). Third, note that the values of the time constant governing the rise of VOR gain from resting to active values showed considerable intertrial and intersubject variability. The effects of this variability are largely tempered, however, by contributions from the SP offset pathway, which start to influence the response after ~110 ms; the overall effect was over within 300 ms.

Figure 9*A* shows a typical visually enhanced VOR onset and offset response and the corresponding model simulation (with parameters for the SP component set at the mean optimal values for this subject and the VOR parameters set at the optimal values for this response). The model successfully simulates the subject's response, including the $\dot{G}$ perturbation at the onset of head rotation exceeding that at offset. The model was similarly successful in this regard for all four subjects. Comparisons between model simulations (calculated using appropriate optimal parameter values) and actual responses of our subjects' visually enhanced VOR were made by computing average residuals waveforms (see METHODS). Inspection of these data (Fig. 9*B*) showed that coherent deviations between model simulations and subject responses were minimal at the onset and offset of head rotation. For leftward head rotations, only *subject 3* showed a residual indicating a gaze velocity lower than model predictions, and this did not exceed 15% of the magnitude of the stimulus.

When we compared each subject's visually enhanced VOR responses with the corresponding model simulations within the critical regions of each response (i.e., the 1st 100 ms after an intended change in chair velocity) using correlation analysis, the correlation coefficient was >0.975. Thus we were able to justify incorporating this model for the visually enhanced VOR into our overall model for CEHT.

SYNTHESIS OF THE CEHT MODEL. We created a model for CEHT by combining the SP onset model with the model of the visually enhanced VOR. This combined model, depicted in Fig. 10, was based on the hypothesis that a linear superposition of the SP and VOR signals generates the observed eye movement signals during CEHT. Notice that the visual input to the model is now relative target velocity [velocity of the target with respect to current gaze velocity, $\dot{T} - \dot{G}$, or $\dot{T} - (\dot{H} + \dot{E})$], which equals $\dot{e}$ (retinal image velocity). However, the brain's internal recreation of target velocity ($\dot{T}'$) is actually a close approximation to absolute target velocity, $\dot{T}$.[1] As before, if the magnitude of $\dot{T}'$ fell below some threshold velocity, the model switched from the SP onset to the SP offset pathway. Thus SP onset provides signals in response to target motion, whereas SP offset contributes to maintenance of fixation when the target is stationary. Finally, the eye movement command signals from the SP and VOR component models were summed according to the superposition hypothesis, and the common command signal was fed to the ocular motor plant.

Testing the superposition model for CEHT

After verifying the validity of each component of the CEHT model, we were next able to test the model (and its underlying hypothesis of SP-VOR superposition) by comparing its simulations with subjects' data collected during various CEHT paradigms.

CHAIR BRAKE. A typical response to the chair-brake stimulus is summarized in Fig. 11*A*. As the subject's head came to a halt, eye movements were initiated promptly as demonstrated by the deflection of $\dot{E}$ at the 2.0-s point in the response. This result is qualitatively similar to that reported

[1] In the model shown in Fig. 10, note that, although the input to the SP system is relative target velocity ($\dot{T} - \dot{G}$), the brain's internal recreation of target velocity ($\dot{T}'$) is actually a reconstruction of absolute target velocity. In fact, the degree to which $\dot{T}'$ deviates from $\dot{T}$ is roughly equivalent to the degree to which $-\dot{E}'_{VOR}$ deviates from $\dot{H}$. This can be seen from the following: $\dot{T}'$ is created internally as the sum of the (delayed) values $\dot{E}'_{SP}$ and the system error signal, $\dot{e}$. This error signal is constructed as $\dot{T} - \dot{H} - \dot{E}$. But, because $\dot{E} = \dot{E}'_{VOR} + \dot{E}'_{SP}$ (assuming the dynamics of the plant to be negligible; see text), then $\dot{e} = \dot{T} - \dot{H} - \dot{E}'_{VOR} - \dot{E}'_{SP}$, and thus $\dot{T}' = \dot{E}'_{SP} + \dot{T} - \dot{H} - \dot{E}'_{VOR} - \dot{E}'_{SP}$. Simplifying, $\dot{T}' = \dot{T} - \dot{H} - \dot{E}'_{VOR}$. The nature of the VOR causes $\dot{E}'_{VOR}$ to be approximately equal and opposite to $\dot{H}$; therefore, $\dot{T}' \approx \dot{T}$.

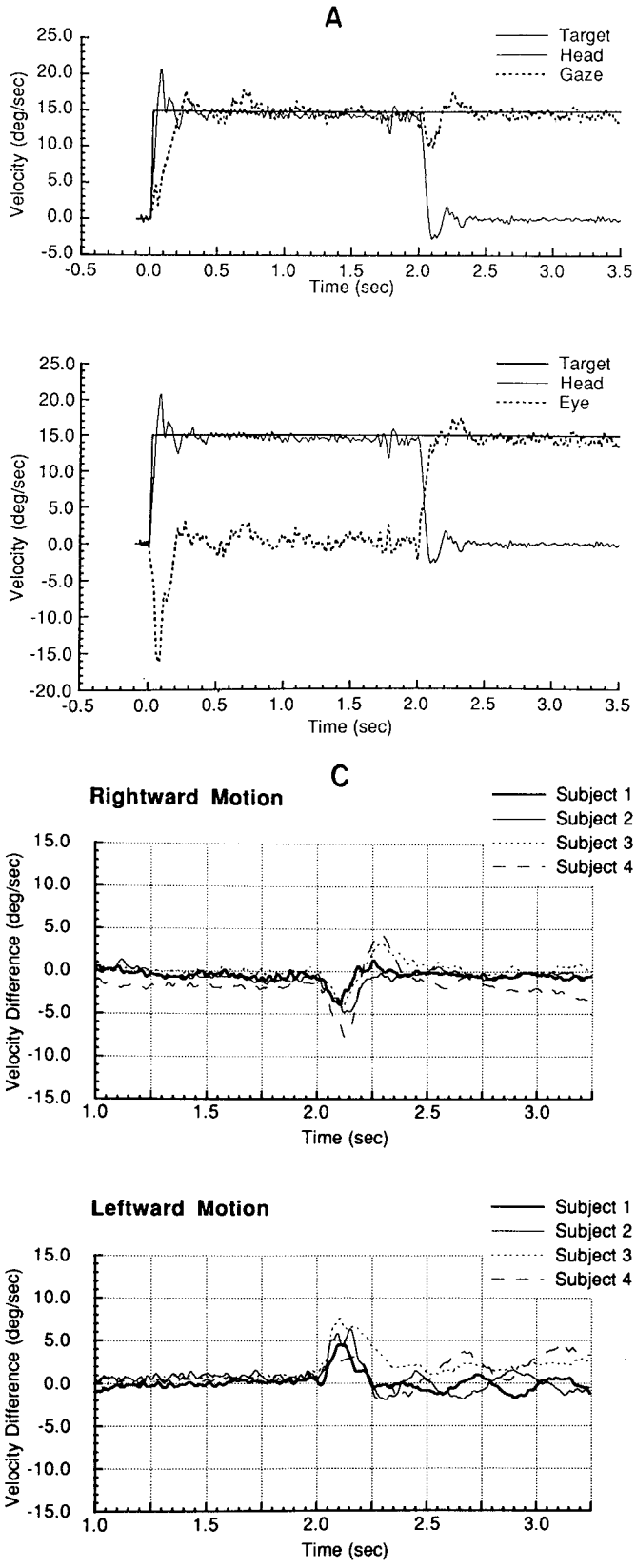

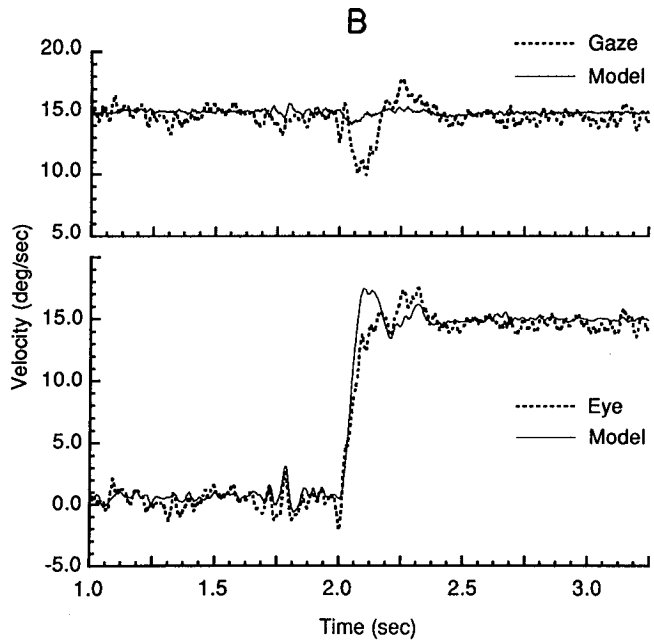

FIG. 11. Chair-brake stimulus. *A*: result from 1 trial in a normal human subject. Eye-in-orbit velocity (eye) and gaze velocity are plotted separately for clarity. At beginning of trial, the chair in which the subject sits (with head fixed to chair) begins to rotate at 15°/s; subject is required to track a target light that moves along with the chair. Gaze soon matches target, and eye-in-orbit movements are minimal. When chair is unexpectedly braked (head velocity falls to 0), eye movements are promptly initiated. Note, however, that gaze velocity does not initially match target velocity. Thus, although a SP signal has likely been active during the initial period of CEHT, the perturbation of gaze velocity at the brake implies that VOR gain has been reduced. *B*: comparison of response of a subject to chair-brake stimulus and corresponding simulation of the response by the CEHT model (shown in Fig. 10), using optimal parameters for this subject. Note how the model accurately predicts prompt onset of eye movements at the onset of the brake but that the subject's gaze is perturbed greater than the model predicts. *C*: comparison between model simulations and subjects' responses for chair-brake stimulus, made by computing average residual waveforms. Positive velocity values indicate that the mean subject's response exceeded the model's predictions. Deviations between model simulations and subject responses were most marked just after the onset of the chair brake, reflecting the gaze perturbation shown by subjects but not predicted by model.

by Lanman et al. (1978). Figure 11*B* shows both the subject response and the corresponding model simulation for the segment of the data in which the chair was braked. On the basis of this close correspondence between subject data and model simulation, we infer that the immediate eye movements seen when the chair is braked are derived from the SP signal because *1*) the model predicted the prompt onset of the eye movements, and *2*) the only signal of suffi-

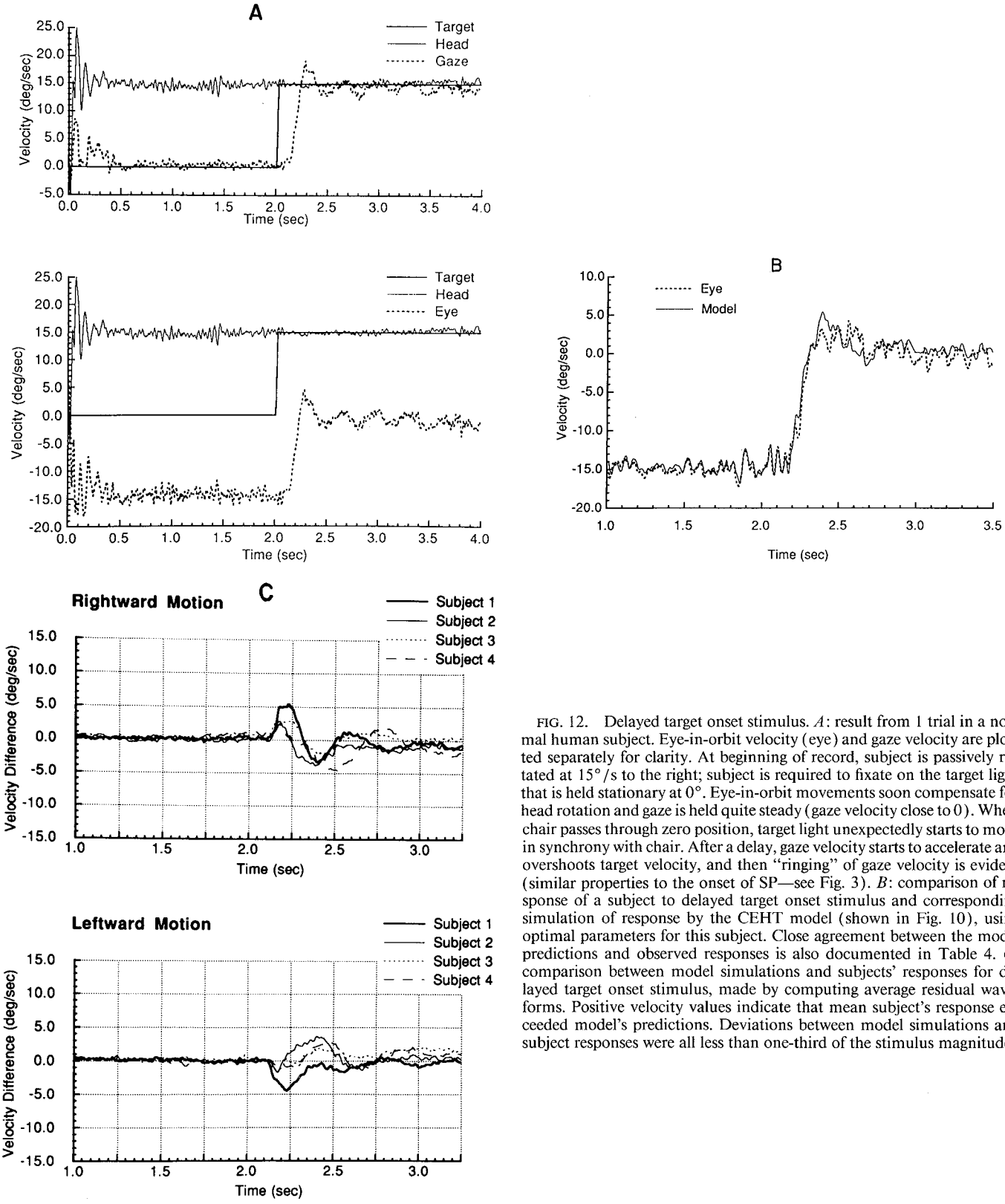

FIG. 12. Delayed target onset stimulus. *A*: result from 1 trial in a normal human subject. Eye-in-orbit velocity (eye) and gaze velocity are plotted separately for clarity. At beginning of record, subject is passively rotated at 15°/s to the right; subject is required to fixate on the target light that is held stationary at 0°. Eye-in-orbit movements soon compensate for head rotation and gaze is held quite steady (gaze velocity close to 0). When chair passes through zero position, target light unexpectedly starts to move in synchrony with chair. After a delay, gaze velocity starts to accelerate and overshoots target velocity, and then "ringing" of gaze velocity is evident (similar properties to the onset of SP—see Fig. 3). *B*: comparison of response of a subject to delayed target onset stimulus and corresponding simulation of response by the CEHT model (shown in Fig. 10), using optimal parameters for this subject. Close agreement between the model predictions and observed responses is also documented in Table 4. *C*: comparison between model simulations and subjects' responses for delayed target onset stimulus, made by computing average residual waveforms. Positive velocity values indicate that mean subject's response exceeded model's predictions. Deviations between model simulations and subject responses were all less than one-third of the stimulus magnitude.

cient magnitude active within the model at the time of the brake that could account for the observed eye movements was generated within the SP system. It can be noted, however, that whereas before the chair brake $\dot{G}$ closely matched $\dot{T}$ (15°/s), afterward $\dot{G}$ temporarily fell to ~11°/s and did not return to 15°/s for an additional 100 ms. Thus, although the unmasked SP command signal provided for immediate movement of the eyes, initial $\dot{E}$ was ~30% less than $\dot{T}$. This finding was different from model simulations, which did not predict a decline of $\dot{G}$ immediately after the

TABLE 4. *Mean eye and model latency* and acceleration† data for responses to the delayed target onset paradigm*

	Subject 1	*Subject 2*	*Subject 3*	*Subject 4*
Rightward motion				
Eye latency	0.137 ± 0.008	0.134 ± 0.017	0.119 ± 0.008	0.159 ± 0.011
Model latency	0.152 ± 0.007	0.160 ± 0.011	0.145 ± 0.005	0.165 ± 0.009
Difference	−0.015 ± 0.008	−0.026 ± 0.016	−0.026 ± 0.011	−0.005 ± 0.004
P	0.0001	0.0013	0.0000	0.0025
Leftward motion				
Eye latency	0.130 ± 0.006	0.150 ± 0.013	0.146 ± 0.015	0.155 ± 0.014
Model latency	0.150 ± 0.010	0.161 ± 0.011	0.151 ± 0.015	0.160 ± 0.009
Difference	−0.020 ± 0.011	−0.011 ± 0.013	−0.006 ± 0.004	−0.005 ± 0.008
P	0.0000	0.0318	0.0012	0.2297
Rightward motion				
Eye accel.	148.0 ± 22.3	85.0 ± 20.8	93.7 ± 20.4	91.7 ± 14.9
Model accel.	123.5 ± 3.5	118.1 ± 7.2	89.3 ± 6.3	103.7 ± 6.5
Difference	24.5 ± 23.9	−33.1 ± 22.8	4.4 ± 17.7	−12.0 ± 16.7
P	0.0067	0.0024	0.4465	0.0496
Leftward motion‡				
Eye accel.	105.7 ± 22.5	86.2 ± 17.0	93.6 ± 16.4	101.0 ± 18.2
Model accel.	90.3 ± 5.4	109.0 ± 6.3	95.6 ± 12.7	99.0 ± 9.3
Difference	15.3 ± 22.5	−22.8 ± 16.9	−2.0 ± 11.2	2.0 ± 12.5
P	0.0381	0.0021	0.6113	0.7159

* Latency data are in seconds; † acceleration data are in deg/s^2; ‡ leftward acceleration values shown as positive.

onset of the brake (Fig. 11*B*). Later in this section we will offer a possible explanation for this discrepancy.

Displaying the average residual waveforms (Fig. 11*C*) facilitated comparison of each subject's responses with model predictions. These plots show that although there was generally good agreement, the model failed to predict the 30% difference between $\dot{E}$ and $\dot{T}$ immediately after the chair brake. Nevertheless, the generally strong similarity of the data and the model predictions was confirmed using correlation analysis, which compared $\dot{E}$ and the model prediction of it, over the 100-ms period after onset of the brake in chair motion. This computation yielded a correlation coefficient >0.95 for all subjects' responses.

Just how good is a 0.95 correlation coefficient? A possible alternative hypothesis of VOR cancellation, in which SP does not sum directly with the VOR command signal, would require the SP system to start from rest when the chair is braked and target motion continues alone. To test the plausibility of this alternative hypothesis, we artificially shifted the model's response 75 ms with respect to $\dot{E}$ [a minimum latency period for human visual tracking (Gellman et al. 1990)] and recalculated correlation coefficients; values were always below 0.66, and were significantly less ($P < 0.0004$) than unshifted comparisons. Shifting to longer, more realistic latencies would have yielded even lower correlation values. Thus simulation behavior closest to actual subject response behavior is that in which the latency between the brake and the subsequent compensatory eye movement is a minimum. These results are obtained when the SP signal is summed directly with the VOR signal. Thus results from the chair-brake experiments do not refute our hypothesis that the SP system provides the primary signal responsible for canceling the VOR during CEHT; however, the deflection of $\dot{G}$ that occurs when the chair is braked suggests that another mechanism may be contributing as well.

What might be the cause of the ~30% perturbation in $\dot{G}$ when the chair was braked? Recall that we encountered a significant perturbation of $\dot{G}$ at the onset of the visually enhanced VOR, but not at the offset (Fig. 4). To account for this finding, we reasoned that VOR gain may change dynamically during the visually enhanced VOR response, being lower at the onset of the head rotation than at the offset. Similarly, the observed gaze perturbation after the brake suggested to us that VOR gain may have fallen back to its resting level (mean value 0.76) during the 2.0-s period of CEHT. Because the VOR is canceled by an active SP signal during CEHT, a VOR with a lower gain would require a lower-amplitude SP signal to cancel it. Then, when the chair was stopped, the active but attenuated SP signal would cause an immediate eye movement but with a velocity less than that of the target, resulting in a perturbation of gaze. Thus, although SP is active during CEHT, its signal is smaller than target velocity. This is evident by the pursuit eye movement produced immediately after the chair brake, which is ~30% less than target velocity (Fig. 11).

DELAYED TARGET ONSET. A typical response to the delayed target onset stimulus is summarized in Fig. 12*A*. Before the onset of target motion, $\dot{E}$ compensates for $\dot{H}$ and, for this visually enhanced VOR, $\dot{G}$ is near zero and there is no ringing. (Recall that "ringing" is a common characteristic of signals created in the SP onset pathway.) After the target starts to move, a delay is evident before $\dot{G}$ starts to accelerate. After $\dot{G}$ matches $\dot{T}$, ringing commences. Thus the onset of CEHT after the visually enhanced VOR is qualitatively similar to the onset of SP (Figs. 3 and 8).

Comparison of each subject's responses with model predictions showed generally good agreement (Fig. 12*B*); some differences between the predicted and observed onset of CEHT were noted, however, particularly in terms of the latency of the response to the initiation of target motion. The average residual waveforms for the delayed target onset paradigm are shown in Fig. 12*C*. Note the near-zero values of the residuals for approximately the first 120 ms after the onset of target motion (at 2.0 s), suggesting close corre-

spondence between subject data and model simulations in this critical response period. Analysis of the latency to the onset of CEHT (Table 4) showed shorter values in subject response data than in model predictions (average difference: 14 ms). This difference was statistically significant ($P < 0.03$) for all subjects, except *subject 4* in a leftward direction, and was responsible for the maximum deflection of $\sim 5°/s$ (about one-third the total stimulus magnitude) in the residual waveforms. On the other hand, average eye acceleration showed no consistent differences between model and data, although in *subject 1* accelerations were significantly greater ($P < 0.04$) and in *subject 2* significantly smaller ($P < 0.003$) than predicted by the model.

A correlation analysis comparing $\dot{E}$ and the model prediction of it confirmed that for the 350- to 400-ms period after the onset of target motion, there was close agreement with a correlation coefficient >0.95 for all subjects' responses. Thus support for the superposition hypothesis was provided by the similarities between subject data and model simulations for the delayed target onset paradigm, specifically with respect to eye acceleration and the presence of ringing in response to the onset of target motion. Only the latency to onset of CEHT after the initiation of target motion differed from that predicted by the model.

DISCUSSION

We have tested the hypothesis, in the form of a mathematical model, that the control of gaze during CEHT is accomplished by a linear superposition of a SP signal with the VOR. Our strategy was *1*) to develop separate models that describe the dynamic properties of SP and vestibular responses of our subjects; *2*) to combine the SP and vestibular models into a model for CEHT in which the eye movement signal is obtained by the linear summation from these two components; *3*) to test the superposition hypothesis by comparing predictions of the CEHT model and subjects' responses to experimental stimuli that were not employed in the development of either constituent model (the chair-brake and delayed target onset paradigms). In this way, we were able to directly test the validity of the superposition hypothesis for CEHT. Our findings indicate that, in humans, an internal SP signal is the primary means by which the VOR is canceled during passive CEHT but that, in addition, a parametric change in VOR gain may contribute to the observed eye movement behavior.

Strong evidence that an internal SP signal cancels the VOR during CEHT comes from the results of the brake experiment. Like Lanman et al. (1978), we found that eye movements commenced promptly when the subjects' heads were stopped. Because the latency to onset of SP is >75 ms, we deduced that a SP signal was initiated during CEHT and, most likely, was used to cancel the VOR. This presence of an active SP signal caused the deflection of eye velocity immediately after the brake onset; its magnitude was, however, smaller than the preceding gaze velocity during CEHT, suggesting that an additional factor was acting to null the VOR.

During the delayed target onset paradigm, ringing of $\dot{G}$ was not noted before the onset of target motion, whereas it was common afterwards. This latter finding supports our model's topology: a "SP offset" (or "fixation") system that generated no ringing supplemented the visually enhanced VOR, but a "SP onset" system that caused "ringing" was activated during CEHT. After the onset of target motion, the latency to onset of CEHT was, on average, ~14 ms shorter than that of SP, a finding that deserves further study.

If cancellation by an internal SP signal is not the sole mechanism by which the VOR is nulled during CEHT, what other possibilities exist? One possibility is that VOR gain is modulated (reduced) during CEHT. Modulation of the gain of the VOR by mental set of the subject is well established (Barr et al. 1976). In our experiments that examined the visually enhanced VOR, we observed dissimilar degrees of gaze perturbation between the onset and offset of head motion. The only way we could satisfactorily explain this phenomenon was that VOR gain increased from a resting level of near 0.75 to an active level of ~0.95 after the initiation of head motion. One advantage of having a lower VOR gain is that it can be more easily overridden during CEHT. Studies from human subjects who have lost vestibular function indicate that the VOR is not necessary for clear and stable vision during stationary activities; only during locomotion do head perturbations demand a VOR with a gain close to 1.0 for vision to remain clear (Leigh et al. 1992). The increase of gain that occurred in our subjects after the onset of a head rotation was achieved too rapidly to be accounted for by visual mechanisms and suggested that VOR gain is influenced by vestibular inputs. A similar rapid increase in VOR gain at the onset of head rotation has also been observed by Gauthier and Vercher (1990).

To explain the increased degree of gaze perturbation after the brake in head movement, we postulate that VOR gain may change dynamically during CEHT; this has been suggested as a possible mechanism in monkey by Lisberger (1990). Specifically, the brain may respond to its reconstruction of relative head movement ($\dot{H}$ with respect to $\dot{T}$) rather than $\dot{H}$ alone when setting its VOR gain value. Neurophysiological evidence suggests that populations of neurons exist that could be the substrate of such a mechanism by responding to $\dot{G}$ during both SP and CEHT and also by receiving vestibular signals. One example is cells in secondary visual areas in the cerebral cortex (Thier and Erickson 1990). Neurons in the cerebellum may also contribute to such a computation (Lisberger 1990).

Do our present findings exclude other mechanisms for overriding the VOR during CEHT? A VOR self-cancellation mechanism, as proposed by Tomlinson and Robinson (1981), could account for our findings if it were the means by which the VOR gain was reduced during CEHT. Cullen and colleagues (1991) found an attenuation of the magnitude of the expected eye movements in response to a head perturbation if their subjects (squirrel monkeys) were engaged in CEHT. They suggest that this result, which is similar to that of our human subjects, might reflect a self-cancellation pathway. On the other hand, Cullen and colleagues (1991) found no such attenuation if the monkey was not engaged in CEHT (i.e., during the visually enhanced VOR). This latter result is different from our human subjects, who did show an attenuation in eye movements, manifested as a perturbation of gaze, that was not

present when the head was later stopped. This difference may be attributable to interspecies differences. For example, the gain of the VOR of the rhesus monkey is close to 1.0 even in darkness (Collewijn 1989; Keller 1978) and does not, as in humans, decline to ~0.65 (Barr et al. 1976).

Our results support a proposal by Lisberger (1990) that more than one mechanism might contribute to gaze modulation during CEHT. Moreover, test conditions may determine which mechanism principally operates. For example, during active head rotations, cancellation of the VOR by an internal SP signal might be the predominant or sole mechanism (Barnes and Lawson 1989; Leigh et al. 1987). Alternatively, an intended head-tracking command might act to null the VOR (Robinson 1982). During passive rotation of subjects in a vestibular chair, however, a VOR self-cancellation mechanism might assume more importance. Furthermore, the mechanism for nulling the VOR during CEHT may be different for different axes of head rotation. For example, in the torsional plane, where there is no SP and only a weak optokinetic response, cancellation of the VOR by visual tracking mechanisms seems unlikely (Leigh et al. 1989). Finally, if more than one mechanism does act to null the VOR during CEHT, then this may account for reports of different properties of SP and CEHT at high rotational frequencies (Kasteel-van Linge and Maas 1990) and discrepant effects of neurological lesions or drugs on SP and CEHT (Chambers and Gresty 1983; Mai et al. 1986). By applying specific quantitative models of the VOR and SP and using the techniques of parameter estimation, it should be possible to elucidate the underlying mechanisms in these other cases of CEHT.

We are grateful to Drs. E. N. Bruce and G. M. Saidel for advice and to O. S. King for technical assistance.

This work was supported by National Eye Institute Grant EY-06717 and NASA grant NA-G9-571 (to R. J. Leigh), the Department of Veterans Affairs, and the Evenor Armington Fund. The work reported in this paper constitutes a portion of the research performed by W. P. Huebner as part of the requirements for his doctoral dissertation.

Present address of W. P. Huebner: KRUG Life Sciences, Houston, TX 77058.

Address for reprint requests: R. J. Leigh, Dept. of Neurology, University Hospitals, 2074 Abington Rd., Cleveland, OH 44106.

Received 26 December 1991; accepted in final form 23 June 1992.

REFERENCES

BAHILL, A. T. AND MCDONALD, J. D. Frequency limitations and optimal step size for the two-point central difference derivative algorithm with applications to human eye movement data. *IEEE Trans. Biomed. Eng.* 30: 191–194, 1983.

BARNES, G. R., BENSON, A. J., AND PRIOR, A. R. J. Visual-vestibular interaction in the control of eye movement. *Aviat. Space Environ. Med.* 49: 557–564, 1978.

BARNES, G. R. AND LAWSON, J. F. Head-free pursuit in the human of a visual target moving in a pseudo-random manner. *J. Physiol. Lond.* 410: 137–155, 1989.

BARR, C. C., SCHULTHEIS, L. W., AND ROBINSON, D. A. Voluntary, nonvisual control of the human vestibulo-ocular reflex. *Acta Otolaryngol.* 81: 365–375, 1976.

BÜTTNER, U. AND WAESPE, W. Vestibular nerve activity in the alert monkey during vestibular and optokinetic nystagmus. *Exp. Brain Res.* 41: 310–315, 1981.

CARL, J. R. AND GELLMAN, R. S. Human smooth pursuit: stimulus-dependent responses. *J. Neurophysiol.* 57: 1446–1463, 1987.

CHAMBERS, B. R. AND GRESTY, M. A. The relationship between disordered pursuit and vestibulo-ocular reflex suppression. *J. Neurol. Neurosurg. Psychiatry* 46: 61–66, 1983.

CHUBB, M. C., FUCHS, A. F., AND SCUDDER, C. A. Neuron activity in monkey vestibular nuclei during vertical vestibular stimulation and eye movements. *J. Neurophysiol.* 52: 724–742, 1984.

COHEN, B., HENN, V., RAPHAN, T., AND DENNETT, D. Velocity storage, nystagmus, and visual-vestibular interactions in humans. *Ann. NY Acad. Sci.* 374: 421–433, 1981.

COLLEWIJN, H. Eye- and head movements in freely moving rabbits. *J. Physiol. Lond.* 266: 471–498, 1977.

COLLEWIJN, H. The vestibulo-ocular reflex: is it an independent subsystem? *Rev. Neurol. Paris* 145: 502–512, 1989.

CULLEN, K. E., BELTON, T., AND MCCREA, R. A. A non-visual mechanism for voluntary cancellation of the vestibulo-ocular reflex. *Exp. Brain Res.* 83: 237–252, 1991.

GAUTHIER, G. M. AND VERCHER, J.-L. Visual vestibular interaction: vestibulo-ocular reflex suppression with head-fixed target fixation. *Exp. Brain Res.* 81: 150–160, 1990.

GELLMAN, R. S., CARL, J. R., AND MILES, F. A. Short latency ocular-following responses in man. *Visual Neurosci.* 5: 107–122, 1990.

GOLDSTEIN, H. P. *The Neural Encoding of Saccades in Rhesus Monkey* (PhD dissertation). Baltimore, MD: Johns Hopkins University, 1983.

GOLDSTEIN, H. P. Modelling post-saccadic drift: dynamic overshoot may be passive. In: *Proceedings of Thirteenth Annual Northeast Biomedical Engineering Conference,* edited by K. R. Foster. New York: IEEE, 1987, vol. 1, p. 245–248.

GROSSMAN, G. E., LEIGH, R. J., ABEL, L. A., LANSKA, D. J., AND THURSTON, S. E. Frequency and velocity of rotational head perturbations during locomotion. *Exp. Brain Res.* 70: 470–476, 1988.

GROSSMAN, G. E., LEIGH, R. J., BRUCE, E. N., HUEBNER, W. P., AND LANSKA, D. J. Performance of the human vestibuloocular reflex during locomotion. *J. Neurophysiol.* 62: 264–272, 1989.

HARY, D., OSHIO, K., AND FLANAGAN, S. D. The ASYST software for scientific computing. *Science Wash. DC* 236: 1128–1132, 1987.

HUEBNER, W. P. AND LEIGH, R. J. Dynamic modulation of VOR gain during passive head rotation. *Ann. NY Acad. Sci.* 656: 857–860, 1992.

HUEBNER, W. P., LEIGH, R. J., AND THOMAS, C. W. An adjustment to eye movement measurements which compensates for the eccentric position of the eye relative to the center of the head. *J. Vestib. Res.* 2: 167–173, 1992.

HUEBNER, W. P., SAIDEL, G. M., AND LEIGH, R. J. Nonlinear parameter estimation applied to a model of smooth pursuit eye movements. *Biol. Cybern.* 62: 265–273, 1990.

HUEBNER, W. P., THOMAS, C. W., AND LEIGH, R. J. Digital filter for eye movement signals. *Med. Biol. Eng. Comput.* 26: 328–330, 1988.

KASTEEL-VAN LINGE, A. AND MAAS, A. J. J. Quantification of visuo-vestibular interaction up to 5.0 Hz in normal subjects. *Acta Otolaryngol.* 110: 18–24, 1990.

KELLER, E. L. Gain of the vestibulo-ocular reflex in monkey at high rotational frequencies. *Vision Res.* 18: 311–315, 1978.

KELLER, E. L. AND DANIELS, P. D. Oculomotor related interaction of vestibular and visual stimulation in vestibular nucleus cells in alert monkey. *Exp. Neurol.* 46: 187–198, 1975.

KOENIG, E., DICHGANS, J., AND DENGLER, W. Fixation suppression of the vestibulo-ocular reflex (VOR) during sinusoidal stimulation in humans as related to the performance of the pursuit system. *Acta Otolaryngol.* 102: 423–431, 1986.

KOWLER, E., MARTINS, A. J., AND PAVEL, M. The effect of expectations on slow oculomotor control. IV. Anticipatory smooth eye movements depend on prior target motions. *Vision Res.* 24: 197–210, 1984.

KRAUZLIS, R. J. AND LISBERGER, S. G. A control systems model of smooth pursuit eye movements with realistic emergent properties. *Neural Comput.* 1: 116–122, 1989.

LANMAN, J., BIZZI, E., AND ALLUM, J. The coordination of eye and head movement during smooth pursuit. *Brain Res.* 153: 39–53, 1978.

LAU, C. G. Y., HONRUBIA, V., JENKINS, H. A., BALOH, R. W., AND YEE, R. D. Linear model for visual-vestibular interaction. *Aviat. Space Environ. Med.* 49: 880–885, 1978.

LEIGH, R. J. AND HUEBNER, W. P. Visual and voluntary control of the vestibulo-ocular reflex. In: *The Vestibulo-Ocular Reflex and Vertigo,* edited by J. A. Sharpe and H. O. Barber. New York: Raven, 1993, chapt. 15, p. 185–193.

LEIGH, R. J., MAAS, E. F., GROSSMAN, G. E., AND ROBINSON, D. A. Visual cancellation of the torsional vestibulo-ocular reflex in humans. *Exp. Brain Res.* 75: 221–226, 1989.

LEIGH, R. J., SAWYER, R. N., GRANT, M. P., AND SEIDMAN, S. H. High frequency vestibuloocular reflex as a diagnostic tool. *Ann. NY Acad. Sci.* 656: 305–314, 1992.

LEIGH, R. J., SHARPE, J. A., RANALLI, P. J., THURSTON, S. E., AND HAMID, M. A. Comparison of smooth pursuit and combined eye-head tracking in human subjects with deficient labyrinthine function. *Exp. Brain Res.* 66: 458–464, 1987.

LISBERGER, S. G. Visual tracking in monkeys: evidence for short-latency suppression of the vestibuloocular reflex. *J. Neurophysiol.* 63: 676–688, 1990.

LUEBKE, A. E. AND ROBINSON, D. A. Transition dynamics between pursuit and fixation suggest different systems. *Vision Res.* 28: 941–946, 1988.

MAAS, E. F., HUEBNER, W. P., SEIDMAN, S. H., AND LEIGH, R. J. Behavior of human horizontal vestibulo-ocular reflex in response to high-acceleration stimuli. *Brain Res.* 499: 153–156, 1989.

MAI, M., DAYAL, V. S., TOMLINSON, R. D., AND FARKASHIDY, J. Study of pursuit and vestibulo-ocular cancellation. *Otolaryngol. Head Neck Surg. Tokoyo* 95: 589–591, 1986.

MCKINLEY, P. A. AND PETERSON, B. W. Voluntary modulation of the vestibuloocular reflex in humans and its relation to smooth pursuit. *Exp. Brain Res.* 60: 454–464, 1985.

RAPHAN, T., MATSUO, V., AND COHEN, B. Velocity storage in the vestibulo-ocular reflex arc (VOR). *Exp. Brain Res.* 35: 229–248, 1979.

ROBINSON, D. A. The control of eye movements. In: *Handbook of Physiology. The Nervous System. Motor Control.* Bethesda, MD: Am. Physiol. Soc., 1981, sect. 1, vol. II, chapt. 28, p. 1275–1320.

ROBINSON, D. A. A model of cancellation of the vestibulo-ocular reflex. In: *Functional Basis of Ocular Motility Disorders,* edited by G. Lennerstand, D. S. Zee, and E. L. Keller. Oxford, UK: Pergamon, 1982, p. 5–13.

ROBINSON, D. A., GORDON, J. L., AND GORDON, S. E. A model of the smooth pursuit eye movement system. *Biol. Cybern.* 55: 43–57, 1986.

STEINMAN, R. M. AND COLLEWIJN, H. Binocular retinal image motion during active head rotation. *Vision Res.* 20: 415–429, 1980.

THIER, P. AND ERICKSON, R. G. Vestibular input to visual-tracking neurons in area FST of awake rhesus monkeys. *Soc. Neurosci. Abstr.* 16: 7, 1990.

THOMAS, C. W., HUEBNER, W. P., AND LEIGH, R. J. A lowpass-notch filter for bioelectric signals. *IEEE Trans. Biomed. Eng.* 35: 496–498, 1988.

TOMLINSON, R. D. AND ROBINSON, D. A. Is the vestibulo-ocular reflex canceled by smooth pursuit? In: *Progress in Oculomotor Research,* edited by A. F. Fuchs and W. Becker. Amsterdam: Elsevier, 1981, p. 533–539.

TOMLINSON, R. D. AND ROBINSON, D. A. Signals in vestibular nucleus mediating vertical eye movements in the monkey. *J. Neurophysiol.* 51: 1121–1136, 1984.

WILSON, V. J. AND MELVILL JONES, G. *Mammalian Vestibular Physiology.* New York: Plenum, 1979.